Bull. Natn. Sci. Mus., Ser. C (Geol.), 5 (2), June 22, 1979

Ontogeny and Variation in *Subprionocyclus neptuni*, an Upper Cretaceous Collignoniceratid Ammonite

By

Ikuwo OBATA

Department of Paleontology, National Science Museum, Tokyo 160

Kazushige TANABE

Department of Geology, Kyushu University, Fukuoka 812

and

Masao FUTAKAMI

Toho Junior and Senior Girls High School, Chofu 182

Introduction

The collignoniceratids represent the "Atlantic-Mediterranean ammonite groups", and have been regarded as rare ammonites in the Upper Cretaceous of Japan. However, in consequence of recent works by MATSUMOTO (1959, 1960, 1965) and OBATA (1965), a considerable number of collignoniceratid species have been found in the Upper Cretaceous sequence of Hokkaido and its adjacent areas.

Subprionocyclus neptuni (GEINITZ), to be described in this paper, was established by GEINITZ (1849, pl. 3, fig. 3) as *Ammonites neptuni* from the Turonian of Saxony, Germany. *A. neptuni* has been given a variety of generic names by different authors; *e.g. Prionocyclus* by WOOD (1896) and WRIGHT and WRIGHT (1951); *Prionotropis* by PERVINQUIÈRE (1907) and COLLIGNON (1931); *Oregoniceras* by ANDERSON (1958); and *Subprionocyclus* by WRIGHT and MATSUMOTO (1954). We agree with MATSUMOTO's (1959) opinion that *A. neptuni* should be included in *Subprionocyclus* because of its mode of ribbing and tuberculation.

MATSUMOTO (1959) realized that *S. neptuni* shows a considerable morphological resemblance with some species of *Collignoniceras, Subprionocyclus* and *Reesidites*. Therefore, *S. neptuni* may be important for the study of the phylogeny of Turonian collignoniceratids.

Although the variation and ontogeny of *S. neptuni* have already studied by MATSUMOTO (1959, 1965) and REYMENT (1975), the details of ontogenetic variation of shell characters have not yet been quantitatively examined to our satisfaction.

In this paper, we describe the ontogenetic development and variation of this species on the basis of careful examination of several samples of populations from the Upper Turonian of the Manji area, central Hokkaido.

We also compare the ontogeny and allometric variation of the present species with those of some allied collignoniceratids, discussing the trend of evolution of the Turonian collignoniceratids.

Notes on Stratigraphic and Geographic Distributions

We start by summarizing the stratigraphic and geographic distributions of the species based on previous works and our own up-to-date unpublished data.

According to MATSUMOTO (1959), *S. neptuni* is found in the upper part of the Middle Turonian of England, Germany and adjacent areas of Europe, Madagascar and Japan; in the lower part of the high Turonian of England according to HANCOCK, KENNEDY and WRIGHT (1977). The species is known from the upper part of the *Inoceramus hobetsensis* Zone (approximately Middle Turonian) of the Pombets, Oyubari, Obira, Saku, and Syumarinai areas and *I. teshioensis* Zone (approximately Upper Turonian) of the Yubari (=Hatonosu) area in Hokkaido (MATSUMOTO, 1965). The index map showing the areas, where *S. neptuni* occurs is given in Fig. 1. Fig. 2 shows the stratigraphic occurrence of the selected collignoniceratids in the Turonian

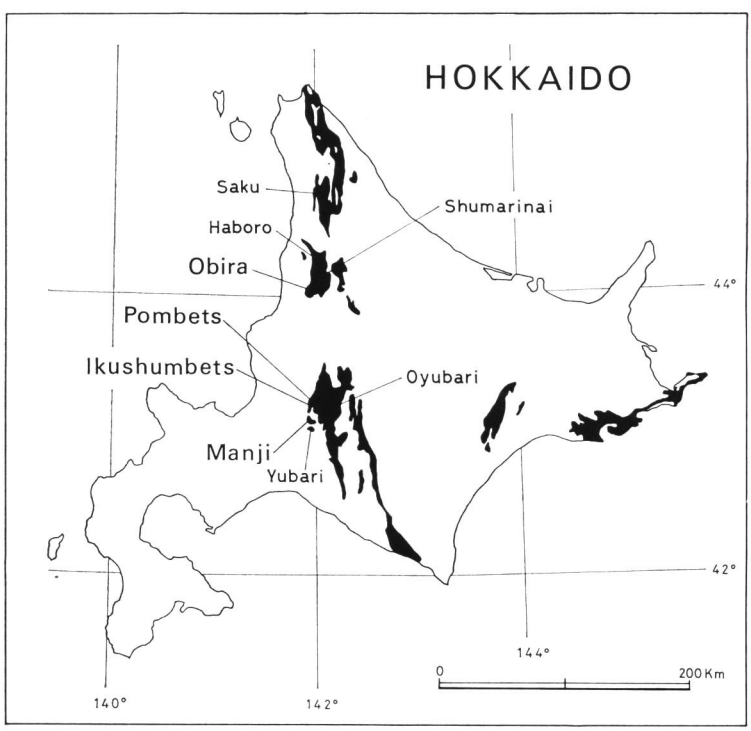

Fig. 1. Map of Hokkaido showing the post-Aptian Cretaceous outcrops (black-shaded) and the areas concerned in this paper.

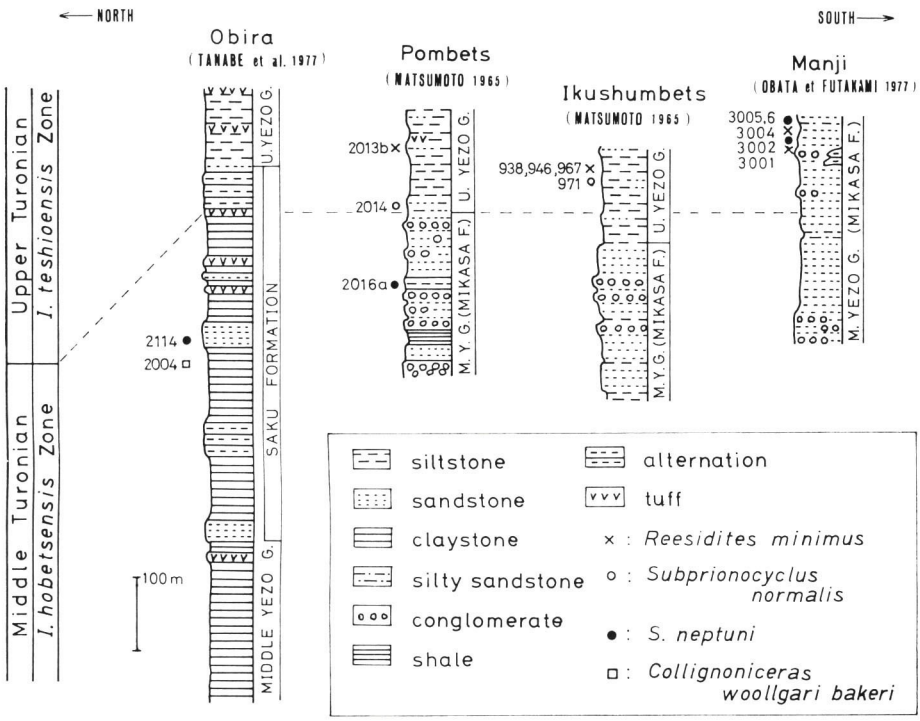

Fig. 2. Stratigraphic columnar sections of the Turonian sequences in selected areas of Hokkaido, with horizons of several important collignoniceratids indicated.

sequence of Hokkaido. As shown in this figure, abundant *S. neptuni* have also been found in the upper part of the Upper Turonian *Inoceramus teshioensis* Zone of the Manji area, central Hokkaido (OBATA and FUTAKAMI, 1977; TANABE *et al.*, 1978).

We have collected *S. neptuni* from the same stratigraphic level as *Reesidites minimus* in the sequence along the Pomporomui of the Manji area in which no hiatus or structural break (fault or folding) is observed, though it has not yet found in the same nodule as *R. minimus*. The geologic route map along the Pomporomui and the neighbouring Aiwoizawa river indicating the stratigraphic occurrence of *S. neptuni* and *R. minimus* in the Upper Turonian is shown in Fig. 3.

In short, *S. neptuni* may be a quite long ranging species from the Middle Turonian to the upper part of the Upper Turonian.

Materials

The present work on *S. neptuni* is based on the examination of the following nine samples from the Upper Turonian of the Manji area (the sample size is indicated in parentheses) (*see* Fig. 3): F1 (5), PM 3F08 (3), PM 3F16 (3), PM 3F17 (3), PM 3F24 (4), PM 3F26 (30), PM 3F27 (4), PM 3F29 (9), PM 3002 (54). Specimens

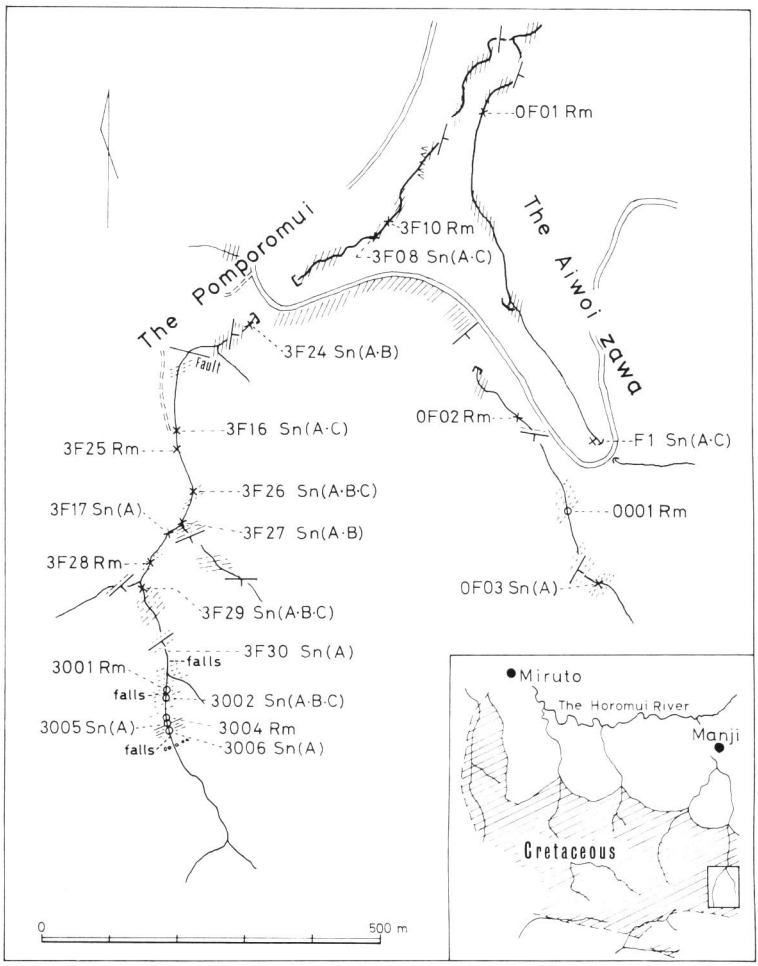

Fig. 3. Geologic route map along the Pomporomui and the Aiwoizawa, tributaries of the Horomui River in the Manji area, central Hokkaido, in which locations of *Subprionocyclus neptuni* (Sn) and *Reesidites minimus* (Rm) are indicated. F number samples (*e.g.* 3F24) are all from float. The occurrence of morphotypes of *S. neptuni* is shown in parentheses. For lithology see the explanation of Fig. 2.

in PM 3002 were carefully separated from a single calcareous sandy nodule embedded in sandstone beds, and those in the remaining eight samples were separated from rolled or fallen nodules in the rivers. These samples were collected by OBATA and FUTAKAMI in 1975–1976, and are now stored in the National Science Museum, Tokyo with the registered numbers beginning NSM. PM.

We have also examined the variation and relative growth of the following five collignoniceratid species on the basis of selected samples.

Collignoniceras woollgari bakeri (ANDERSON): Twenty-five specimens from the Middle Turonian at a locality in the Nakakinembets River, Obira area, northwestern Hokkaido (sample OB).

Subprionocyclus bravaisianus (D'ORBIGNY): Eleven specimens from the Upper Turonian in the Uchaux Basin, Vaucluse, northern France (Uchaux sample).

Subprionocyclus normalis (ANDERSON): Thirteen specimens from the Upper Turonian at loc. CIT 1346, left bank of Little Cow Creek, Shasta County, California (sample CIT 1346).

Reesidites minimus (HAYASAKA and FUKADA): Thirty six specimens from the Upper Turonian at loc. IK 946, near Katsurazawa Dam, Ikushumbets area, central Hokkaido (sample IK 946); fourteen specimens from the Upper Turonian at loc. IK 938, near Katsurazawa Dam (sample IK 938); fourty-five specimens from the Upper Turonian at loc. SN 2F01 (a floating sample) in the upper stream of the Sannosawa, Manji area (SN 2F01 sample); twenty-eight specimens from the Upper Turonian at loc. RN 8001 along the Pomnebets forestry road, Manji area (sample RN 8001); sixty specimens from the Upper Turonian at loc. SN 2003 in the upper stream of the Sannosawa, Manji area (sample SN 2003).

Reesidites elegans MATSUMOTO and INOMA: Seven specimens separated from loose nodules at loc. 71905 in the upper reaches of the Haboro river, Haboro area, northwestern Hokkaido (W. HASHIMOTO coll.; Haboro sample). These specimens are kept in Tokyo Kyoiku University (now University of Tsukuba) with registered numbers beginning prefix TKU. MATSUMOTO and INOMA (1971, *in* MATSUMOTO, 1971) described this species with measurements on these specimens which are used in this paper. According to them, the source beds of these specimens are interpreted as Upper Turonian.

For the Californian sample of *S. normalis*, MATSUMOTO's (1960, p. 113) measurements are used here. Eleven specimens of *S. bravaisianus* are kept at the Institut de Paléontologie, Muséum National d'Histoire Naturelle, Paris. MATSUMOTO and NODA (1966) studied these specimens taxonomically and gave the quantitative data which are adopted in this paper. The measurements on specimens of the remaining two species were performed by OBATA and FUTAKAMI. Two samples of *R. minimus* with the prefix IK were collected by MATSUMOTO, and are now deposited in the Type Collection of Kyushu University. The other two samples of *R. minimus*, and the sample of *C. woollgari* were collected by OBATA and FUTAKAMI, and are now stored in the National Science Museum.

Method of Study

Measurements: The following shell characters have been examined in the study of ontogenetic development and allometry of *S. neptuni*. Abbreviations used in tables and figures are shown in parentheses: shell diameter (D), whorl height (H) and breadth (B), umbilical diameter (U) and its half length (C), radius of a spiral (R), siphuncular

diameter (Sd), protoconch width, nepionic size, thickness of ventral wall and septum, number of septa, and numbers of umbilical (UT) and upper ventrolateral (VT) tubercles per whorl.

For the analysis of average relative growth and variation, such characters as D, H, B and U were measured on specimens with a slide caliper of accuracy 0.1 mm. UT and VT per whorl were counted under a WILD microscope on every specimen examined.

The measurements obtained were divided into several size classes in accordance with the shell size of the specimens for the analysis of ontogenetic variation. The study of ontogenetic development of the present species is based on measurements of many characters on a polished median dorso-ventral section or a cross section of several specimens selected from sample PM 3002. For this purpose, the radius of a spiral, number of septa, and thickness of the ventral wall and septum were measured on a median section at intervals of $0.5\,\pi$.

Whorl height and breadth, shell diameter, umbilical diameter and its half length, siphuncular diameter, and the thickness of the shell wall were measured in a cross section at intervals of 1π.

Measurements on median and cross sections were carried out by TANABE with an aid of a profile projector microscope (Nippon Kogaku Co.) of 1 μm accuracy, with a digital printer.

We also calculated the parameters of RAUP and MICHELSON (1965), namely the whorl expansion rate ($WR=(R_n/R_{n-1})^2$), the distance of the generating curve from the

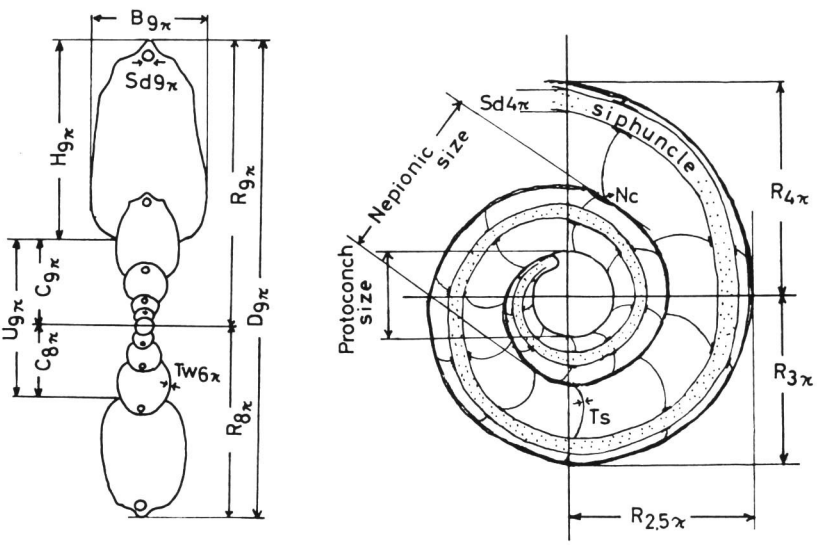

Fig. 4. Diagram showing the basic morphology, orientation and measurements along the median dorsoventral (right half) and cross (left half) sections of *S. neptuni*. For abbreviations in this figure see the explanations in the text. Read R 3.5 π for R 2.5 π.

axis of coiling (DG=C/R), and the form-ratio of the generating curve (S=B/H) to investigate the ontogenetic change of shell-form.

The basic morphology, orientation and measurements of *S. neptuni* are diagrammatically represented in Fig. 4.

Biometry: We have analysed the ontogeny and variation of the present species with some biometric treatment. The following abbreviations were used for biometry.

N: number of specimens in a sample, O. R.: observed range, $\overline{X}$: arithmetic mean, V: coefficient of variation, s: standard deviation, $\sigma\bar{x}$: standard error of the mean, $\overline{X}\pm t_{0.05}\sigma\bar{x}$: 95% confidence interval of the mean, α: slope (=growth ratio) of allometric equation, β: initial growth index of allometric equation, r: correlation coefficient.

Ontogeny

1. Ontogenetic development

The ontogenetic development and variation in the early stage (less than 20 mm in shell-diameter) of *S. neptuni* have been examined for several selected specimens of sample PM 3002. Fig. 5 summarizes the results. The basic data of this figure are shown in Tables 1–2.

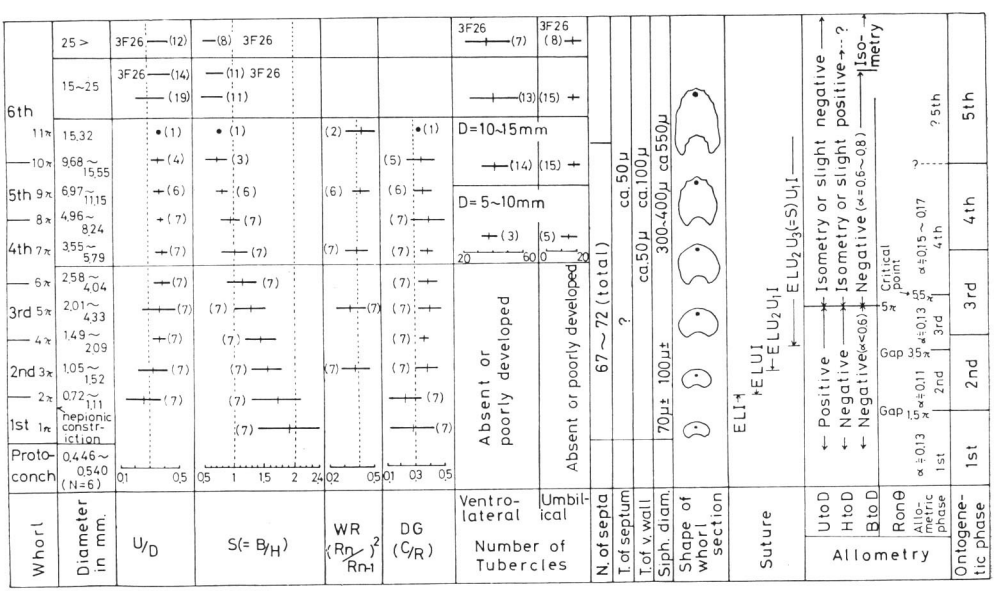

Fig. 5. Ontogenetic development and variation in the early to middle growth stages of *S. neptuni* based on the examination of selected specimens in samples PM 3002 and PM 3F26. For the parameters, U/D, S, WR, and DG, the sample mean (cross line) and twice the standard deviation are shown at each growth stage. The sample size is indicated in parentheses. For abbreviations in this figure see the explanations in the text.

Table 1. Variation of several characters at different growth stages in specimens selected from sample PM 3002.

Character	Growth stage (π)	N	$\bar{X}$ in mm	V	s in mm	Observed range in mm
Protoconch width	—	6	0.482	6.9	0.03	0.446—0.540
Shell diameter	2	10	0.88	12.5	0.11	0.716—1.110
	3	10	1.23	11.4	0.14	1.046—1.520
	4	10	1.70	11.8	0.20	1.494—2.094
	5	10	2.52	27.8	0.70	2.006—4.334
	6	10	3.23	15.8	0.51	2.576—4.039
	7	10	4.56	16.7	0.76	3.550—5.792
	8	10	6.40	16.9	1.08	4.964—8.242
	9	9	8.88	15.7	1.39	6.974—11.146
	10	5	12.76	19.4	2.47	9.676—15.550
	11	1	15.32			
Whorl breadth	2	6	0.663	9.1	0.06	0.568—0.728
	3	6	0.772	8.4	0.07	0.676—0.872
	4	6	0.910	14.1	0.13	0.688—1.036
	5	6	1.114	6.6	0.07	0.964—1.206
	6	6	1.357	12.5	0.17	1.212—1.614
	7	6	1.817	16.2	0.29	1.348—1.992
	8	6	2.000	12.3	0.25	1.796—2.380
	9	6	2.714	18.0	0.49	2.076—3.360
	10	3	3.318	18.3	0.61	2.648—3.830
	11	1	4.560			
Whorl height	2	7	0.369	18.2	0.07	0.250—0.440
	3	7	0.470	13.0	0.06	0.394—0.564
	4	7	0.648	14.8	0.10	0.542—0.762
	5	7	0.855	15.2	0.13	0.686—0.972
	6	7	1.177	21.4	0.25	0.866—1.478
	7	7	1.699	18.5	0.32	1.280—2.036
	8	7	2.350	18.9	0.44	1.794—2.896
	9	6	3.468	20.4	0.71	2.520—4.536
	10	4	4.847	30.1	1.46	3.428—6.716
	11	1	5.820			
Umbilical diameter	2	7	0.236	25.8	0.06	0.128—0.316
	3	7	0.412	19.7	0.08	0.286—0.546
	4	7	0.586	14.7	0.09	0.532—0.818
	5	7	0.918	15.8	0.15	0.746—1.188
	6	7	1.313	17.9	0.24	0.966—1.698
	7	7	1.810	16.8	0.30	1.364—2.302
	8	7	2.500	17.7	0.44	1.906—3.144
	9	7	3.438	17.7	0.61	2.664—4.192
	10	4	4.462	16.8	0.75	3.736—5.140
	11	1	5.514			

Although the ontogenetic change of many characters is more or less continuous, the following five growth-phases are recognized in the early to middle ontogeny of

Table 2. Variation of several parameters at different growth stages in specimens selected from sample PM 3002.

Parameter	Growth stage (π)	N	$\bar{X}$	V	s	Observed range
U/D	2	7	0.26	23.1	0.06	0.147—0.333
	3	7	0.33	15.2	0.05	0.228—0.362
	4	7	0.37	5.4	0.02	0.338—0.380
	5	7	0.37	16.2	0.06	0.237—0.425
	6	7	0.39	7.7	0.03	0.368—0.446
	7	7	0.39	5.1	0.02	0.358—0.419
	8	7	0.38	2.6	0.01	0.377—0.406
	9	6	0.37	5.4	0.02	0.330—0.391
	10	4	0.36	5.6	0.02	0.326—0.386
	11	1	0.36			
S=B/H	1	6	1.93	13.5	0.26	1.746—2.418
	2	7	1.78	12.9	0.23	1.616—2.272
	3	7	1.57	7.0	0.11	1.398—1.730
	4	7	1.43	9.1	0.13	1.246—1.780
	5	7	1.27	10.2	0.13	1.091—1.478
	6	7	1.15	11.3	0.13	0.939—1.312
	7	7	0.97	12.4	0.12	0.851—1.181
	8	7	0.90	8.9	0.08	0.808—1.001
	9	6	0.75	6.7	0.05	0.675—0.824
	10	3	0.67	14.9	0.10	0.570—0.772
	11	1	0.78			
Whorl expansion rate	3	7	1.96	6.6	0.13	1.818—2.199
	5	7	1.87	7.0	0.13	1.696—2.060
	7	7	2.00	4.5	0.09	1.800—2.141
	9	6	2.07	3.4	0.07	1.889—2.120
	11	2	2.10	5.7	0.12	2.018—2.181
Distance of generating curve from axis	1	7	0.28	28.6	0.08	0.170—0.398
	2	7	0.25	24.0	0.06	0.130—0.330
	3	7	0.38	10.5	0.04	0.292—0.416
	4	7	0.36	2.8	0.01	0.340—0.388
	5	7	0.40	10.0	0.04	0.347—0.456
	6	7	0.39	7.7	0.03	0.378—0.439
	7	7	0.39	5.1	0.02	0.366—0.428
	8	7	0.40	15.0	0.06	0.370—0.531
	9	6	0.36	8.3	0.03	0.304—0.396
	10	5	0.35	14.3	0.05	0.280—0.369
	11	1	0.36			

this species on the basis of ontogenetic appearance and growth-pattern of many shell-characters.

The first phase (protoconch and main part of the first whorl): This phase is divided into protoconch and nepionic stages. The protoconch is roughly spherical or ellipsoidal in shape, being partly enveloped by the succeeding first whorl. Its width ranges

from 446 to 540 μm, and the variation in PM 3002 is rather small (V=6.9).

A clear nepionic constriction exists at about the 1.5 π stage, and this makes a pronounced gap in growth of the radius at the same stage (refer to the section on ontogenetic relative growth on p. 61). So far as the specimens examined, the maximum nepionic size is about 1 mm. The whorl is moderately to much depressed, the height being much smaller than the width with the form-ratio (S) of more than 1.7 (*see* Table 2). The number of septa in this phase is 7 to 8. The distance of the generating curve (DG) at the 1 π stage ranges from 0.17 to 0.40 showing a much larger coefficient of variation (V=28.6) than those in the succeeding growth phases. The surface is smooth without any trace of a ventral keel or tubercles. The siphuncular tube is subcentral in this phase. The suture line is expressed by E L I in terms of WEDEKIND's formula.

The second phase (the later part of the first whorl to the second whorl): The diameter is less than 3.0 mm, and the shell is fairly narrowly umbilicate at the 2 π stage, but it becomes fairly widely to moderately umbilicate with growth, showing the decrease in the range of variation (*see* Fig. 5 and Table 2); the umbilicus is shallow with an inclined wall. Whorls are embraced, and fairly depressed, with the form-ratio (S) ranging from 1.25 to 1.78, being smaller than that in the first phase.

It is interesting that the distance of the generating curve (DG) abruptly increases from the 2 π stage to the 3 π stage (*see* Fig. 5.) The siphuncle gradually shifts towards the ventral side during the growth of the second whorl. The surface is still smooth without any ornamentation.

The suture line is expressed as E L I at the beginning part, E L U I at the earlier, E L U_2 U_1 I at the middle, then E L U_2 U_3 (=S) U_1 I at the later.

The third phase (the third and the early part of the fourth whorl): The shell-diameters range from about 1.5 to 5.8 mm. The shell is moderately involute; the umbilicus is moderately wide, being from 24% to 45% of the diameter (*see* Table 2). The umbilical shoulder becomes subrounded with a steep umbilical wall. During this phase at each of several growth-stages, the mean form-ratio (S) gradually decreases with growth from 1.3 to 1.0; thus the whorl becomes higher than broad, increasing more rapidly in height than in breadth. The siphuncle lies on the ventral side.

The whorl-expansion-rate at the 5 π stage is about 1.70 to 2.06; however, it becomes larger with growth from the beginning of the fourth whorl (ca. 7 π).

The variation of the parameter DG is generally small throughout this phase with the constant mean of about 0.4.

Flnaks are smooth without ribbing, but a smooth ventral keel is discernible in the early part of the fourth whorl. The upper ventrolateral (34–38 per whorl) and umbilical (12–18 per whorl) tubercles begin to appear in the later stage of this phase.

The sutural pattern, being expressed by E L U_2 U_3 (=S) U_1 I, is characterized by its V to U-shaped lateral lobe in outline and small dentate lobe incisions.

The fourth phase (the main part of the fourth to the fifth whorl): Diameters are from 4.96 to 15.55 mm. The shell is rather moderate in involution; the umbilicus is

moderately wide to narrow, being from 38% to 41% of the diameter. The range of variation in the ratio U: D during this phase is much smaller than those in the preceding second to third phases. Furthermore, its mean value at each of several stages in this phase gradually decreases with growth, in contrast with the increase during the second to the third phases (*see* Fig. 5 and Table 2). Whorls are more or less compressed with the form-ratio (S) of 0.7 to 0.9, decreasing with growth.

The venter is distinctly keeled on the median line. The keel is serrated, sharp, narrow and prominent. The small, but characteristic lower ventrolateral tubercles tend to appear on ribs together with the already existing upper ventrolateral tubercles at the end of the ribs. The number of paired tubercles is more numerous than the ones on the umbilical shoulder.

Flanks are ornamented with the flexiradiate ribs, which are sometimes bifurcated near the inner flank and there are also some intercalated shorter ribs. The ribs show a gently sigmoidal curvature on the middle flank, and are sharply bent forward at the submarginal inner ventrolateral point where small lower ventrolateral tubercles are well developed.

The number of umbilical tubercles per whorl is almost constant with growth, while the double ventrolateral ones become more numerous with growth (*see* Fig. 5).

The fifth phase after the sixth whorl: Unfortunately, we could not examine in detail the ontogenetic variation in the stage after the sixth whorl, because of insufficient large specimens at our disposal for ontogenetic analysis. However, MATSUMOTO (1959, 1965) has already described qualitatively the variation in the middle to adult stages of the present species.

2 Individual relative growth

To examine the ontogenetic development of this species from the viewpoint of allometry, the individual relative growth of several shell characters has been investigated for several specimens of sample PM 3002.

Growth of radius vector: As shown in Fig. 6, the growth pattern of the radius to the total rotation angle exhibits four allometric growth phases, namely, at 0–1.5 π, 2–3.5 π, 4–5.5 π, 5.5–11 π, during the early to middle stage of the species. The subdivision of allometric growth phase in comparison with that of ontogenetic growth phase is summarized in Fig. 5.

Pronounced gaps in allometric growth exist between both the first and second and between the second and third phases in the specimens examined.

As mentioned before, these gaps may originate in the nepionic constriction at about 1.5 π. The third and fourth phases are bounded by a clear critical point around 5.5 π.

As THOMPSON (1917) and HUXLEY (1932) demonstrated mathematically, the growth of whorls of many cephalopod and gastropod shells displays a logarithmic spiral.

Subsequently, OBATA (1959, 1960) realized that the growth of spiral in some

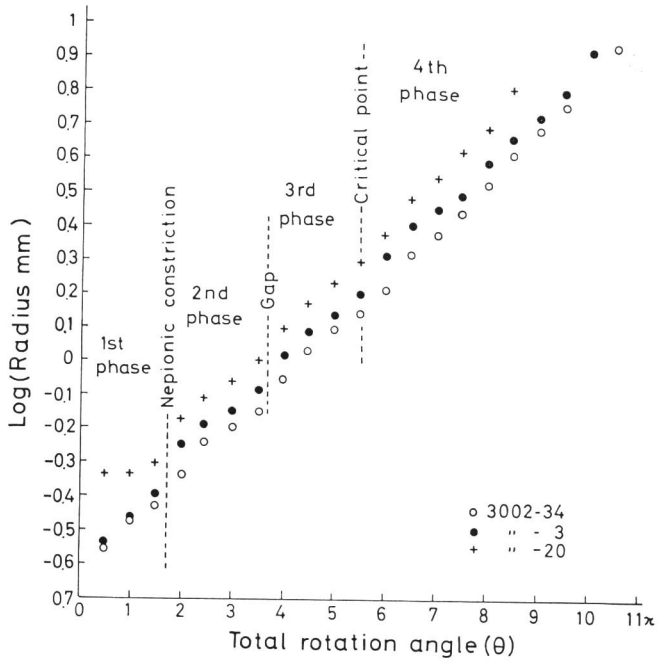

Fig. 6. Individual growth pattern of radius in relation to the total rotation angle in three selected specimens of *S. neptuni* in sample PM 3002.

Cretaceous planispiral ammonoids can be expressed as a function of polar coodinates.

We can approximate the growth of radius (R) in relation to the total rotation angle (θ) in the planispiral ammonoids by the equation, $R=\beta\theta^{\alpha}$, by means of the least squares method; where β and α are the initial growth index and the slope (growth ratio) of an allometric equation respectively.

The calculated allometric equations in the first to the fourth phases for the three speciemens selected from sample PM 3002 are as follows.

Specimen Allometric phases	3002–34 (NSM. PM 7420)	3002–3 (NSM. PM 7389)	3002–20 (NSM. PM 7406)
1st phase	$R=0.2363\theta^{0.1297}$	$R=0.2399\theta^{0.1437}$	——
	$r=0.9831$	$r=0.9999$	
2nd phase	$R=0.2674\theta^{0.1217}$	$R=0.3403\theta^{0.1071}$	$R=0.3994\theta^{0.1128}$
	$r=0.9789$	$r=0.9953$	$r=0.9896$
3rd phase	$R=0.2666\theta^{0.1306}$	$R=0.3602\theta^{0.1163}$	$R=0.3771\theta^{0.1302}$
	$r=0.9891$	$r=0.9961$	$r=0.9965$
4th phase	$R=0.1887\theta^{0.1562}$	$R=0.2529\theta^{0.1485}$	$R=0.2406\theta^{0.1653}$
	$r=0.9991$	$r=0.9953$	$r=0.9965$

The slope in the fourth phase is much steeper than that in the third in these three specimens. This observation may be well explained by the abrupt increase of whorl-expansion-rate after the 6 π stage (*see* Fig. 5).

Growth of whorl height, breadth and umbilical diameter: We have examined the growth of whorl height, breadth and umbilical diameter compared with the shell diameter in the present species with the aid of the reduced major axis method (KERMACK and HALDANE, 1950).

Measured values at different growth stages were plotted on a double logarithmic graph showing the relationship between two characters for each specimen examined. The purpose was to distinguish whether the ontogenetic growth of the above-mentioned three characters is monophasic allometry or polyphasic allometry.

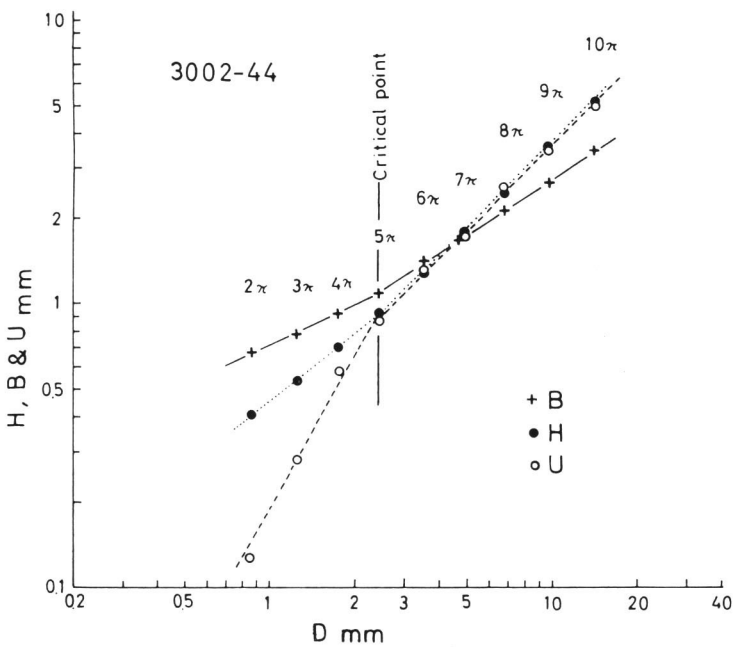

Fig. 7. Double logarithmic scatter-diagram showing the ontogenetic growth of whorl-height and breadth, and umbilical diameter in relation to shell-diameter in specimens PM 3002–44 (NSM. PM 7430). For abbreviations in this figure see the explanations in the text.

As shown in Fig. 7, a clear critical point may exist at about the 5 π stage for the growth of each character in relation to shell diameter; thus the growth pattern of the above mentioned characters represents diphasic allometry.

The results of individual relative growth analysis for several selected specimens are summarized in Table 3. We used the expedient method of HAYAMI and MATSUKUMA (1970) for the discrimination of allometry.

Table 3. Results of individual relative growth analysis by means of the reduced major axis method for certain characters in specimens selected from sample PM 3002.

Early phase (0—5 π)	N	$\bar{\alpha}\pm t_{0.05\sigma\bar{\alpha}}$	$\bar{\beta}\pm t_{0.05\sigma\bar{\beta}}$	s_α	O. R.$_\alpha$	Discrimination of allometry
H to D	7	0.8211±0.1087	0.4070±0.0268	0.12	0.6184—0.9621	slight negative
B to D	6	0.4304±0.1011	0.6934±0.0347	0.10	0.2782—0.5553	negative
U to D	7	1.4635±0.2430	0.2789±0.0522	0.26	1.0959—1.9231	positive
Later phase (5π—11π)	N	$\bar{\alpha}\pm t_{0.05\sigma\bar{\alpha}}$	$\bar{\beta}\pm t_{0.05\sigma\bar{\beta}}$	s_α	O. R.$_\alpha$	Discrimination of allometry
H to D	7	1.0433±0.0561	0.3427±0.0306	0.06	0.9859—1.1608	isometry
B to D	6	0.7090±0.0763	0.5617±0.0702	0.07	0.6493—0.8467	negative
U to D	7	0.9480±0.0775	0.4175±0.0590	0.08	0.7829—1.0410	slight negative

The slope of the reduced major axis for the growth of whorl-height and breadth to shell-diameter changes first from negative allometry to slight positive allometry, and then from strong negative allometry to slight negative allometry with growth. Conversely that of the umbilical diameter to shell diameter changes from positive allometry during the early phase to slight negative allometry during the later one.

Growth of siphuncle: The growth of siphuncular tube diameter in relation to shell diameter in the present species has been analysed in two specimens selected from sample PM 3002 by means of the reduced major axis method again. As a result of this analysis, we distinguished two growth phases in the growth of siphuncular diameter. The allometric equations calculated in the two specimens are as follows.

Specimen	PM 3002–55	PM 3002–44
Growth phase	(NSM. PM 9261)	(NSM. PM 7430)
0–5 π	$SD=0.117D^{0.065}$	$SD=0.090D^{0.486}$
	r=0.9732	r=0.9830
5–10 π	$SD=0.055D^{0.976}$	$SD=0.047D^{1.029}$
	r=0.9843	r=0.9837

A pronounced critical point exists between the two growth phases, and the slope of the reduced major axis changes from negative allometry to isometry with growth. Therefore, the growth pattern of siphuncular diameter is almost harmonious with those of radius vector, whorl breadth and height.

3. Average relative growth

The average relative growth of such characters as umbilical diameter, whorl height and breadth in relation to shell diameter or whorl height in the present species has been examined for the samples PM 3F26, PM 3F29 and PM 3002 with an aid of the reduced major axis method. The basic data of measurements are listed in Table 4.

Of course, the slope and correlation coefficient of an allometric equation may be

Table 4. Measurement data of the examined specimens of *S. neptuni*.

	Specimen	D	H	H/D	B	B/D	B/H	U	U/D (%)	UT	VT	Type*
F1-1	(NSM.PM 7053)	(42.5)	16.4	(0.39)	(10.2)	(0.24)	(0.62)	15.0	(35)	12	(13×2)	C
2	(NSM.PM 6984)	(46.7)	18.1	(0.39)	(11.8)	(0.25)	(0.65)	(18.9)	(40)	12	(25)	C
3	(NSM.PM 7054)	(42.0)	17.6	(0.42)	8.4	(0.20)	0.48	—	—	—	—	
4	(NSM.PM 7077)	32.6	15.7	0.48	—	—	—	8.1	25	15	(35)	
5	(NSM.PM 7068)	39.6	17.1	0.43	—	—	—	11.4	29	13	31	
3F08-1	(NSM.PM 7072)	44.8	17.0	0.38	—	—	—	15.0	33	(7×2)	(14×2)	
2	(NSM.PM 9259)	32.0	14.4	0.45	(7.2)	(0.23)	(0.50)	10.4	33	(7×2)	(16×2)	
3	(NSM.PM 7122)	—	—	—	—	—	—	—	—	(12)	35	
3F16-1	(NSM.PM 7047)	60.1	26.4	0.44	15.0	0.25	0.57	18.2	30	14	27	
2	(NSM.PM 7000)	(61.0)	24.4	(0.40)	18.4	(0.30)	0.75	20.8	(34)	(7×2)	(14×2)	C
3	(NSM.PM 7001)	16.6	6.2	0.37	—	—	—	6.4	39	(7×2)	(19×2)	
3F17-1	(NSM.PM 6978)	18.5	6.7	0.36	—	—	—	7.4	40	(8×2)	(19×2)	
2	(NSM.PM 7002)	27.0	8.8	0.33	5.9	0.22	0.67	10.2	38	—	—	
3	(NSM.PM 7051)	62.2	27.0	0.43	(18.0)	(0.29)	(0.67)	15.6	25	11	(33)	
3F24-1	(NSM.PM 7344)	32.5	13.6	0.42	8.0	0.25	0.59	10.3	31	(7×2)	(17×2)	B
2	(NSM.PM 7345)	17.6	6.7	0.38	—	—	—	7.0	40	22	(45)	
3	(NSM.PM 7346)	19.0	6.0	0.32	(3.1)	(0.16)	(0.52)	7.9	42	19	39	
4	(NSM.PM 7347)	(20.2)	—	—	—	—	—	5.2	(26)	15	38	
3F26-1	(NSM.PM 7301)	39.1	16.8	0.43	(10.8)	(0.28)	(0.64)	10.7	27	10	(26)	
2	(NSM.PM 7302)	26.2	10.0	0.38	6.3	0.24	0.63	10.0	38	16	45	B
3	(NSM.PM 7303)	29.9	11.7	0.39	6.7	0.22	0.57	9.2	31	16	(32)	
4	(NSM.PM 7304)	26.8	10.3	0.38	6.2	0.23	0.60	9.0	34	15	40	
5	(NSM.PM 7305)	28.5	10.9	0.38	7.4	0.26	0.68	10.4	36	19	43	
6	(NSM.PM 7306)	(23.6)	8.8	0.37	6.1	0.26	0.69	(7.6)	(32)	12	34	
7	(NSM.PM 7307)	—	15.6	—	8.8	—	0.56	—	—	—	—	
8	(NSM.PM 7308)	29.5	12.3	0.42	7.1	0.24	0.58	9.1	31	12	27	
9	(NSM.PM 7309)	20.8	9.1	0.44	5.9	0.28	0.65	7.1	34	16	37	
10	(NSM.PM 7310)	(18.1)	7.4	0.41	5.5	0.30	0.74	5.6	(31)	15	31	
11	(NSM.PM 7311)	28.1	10.8	0.34	(6.0)	(0.21)	(0.56)	9.4	33	(16)	(41)	
	(90)	23.6	8.9	0.38	5.5	0.23	0.62	8.5	36	—	—	
12	(NSM.PM 7312)	(34.1)	(14.0)	(0.41)	—	—	—	11.1	(33)	17	39	
13	(NSM.PM 7313)	(33.8)	(12.9)	(0.38)	—	—	—	11.9	(35)	19	(40)	
14	(NSM.PM 7314)	30.8	11.1	0.36	—	—	—	10.7	35	(7×2)	—	
15	(NSM.PM 7315)	13.8	4.3	0.31	(2.0)	(0.14)	(0.47)	5.0	36	(7×2)	(14×2)	C
16	(NSM.PM 7316)	(19.2)	7.6	(0.40)	3.9	(0.20)	0.51	(6.1)	(32)	(12)	(32)	
17	(NSM.PM 7317)	23.1	9.0	0.39	—	—	—	8.0	35	16	(30)	
18	(NSM.PM 7318)	(13.3)	(5.1)	(0.38)	(3.1)	(0.23)	(0.61)	(4.7)	(35)	—	—	
19	(NSM.PM 7319)	16.3	6.2	0.38	(4.1)	(0.25)	(0.66)	5.9	36	14	(18×2)	
20	(NSM.PM 7320)	22.3	8.7	0.39	5.5	0.35	0.63	8.0	36	(7×2)	—	
	(inner vol.)	15.8	5.5	0.35	3.0	0.19	0.55	5.8	37	—	—	
21	(NSM.PM 7321)	15.5	5.7	0.37	3.4	0.22	0.60	5.8	37	16	(38)	
22	(NSM.PM 7322)	18.2	6.8	0.37	—	—	—	5.6	31	13	(33)	
23	(NSM.PM 7323)	17.7	8.0	0.45	5.4	0.31	0.68	(5.0)	28	—	—	
24	(NSM.PM 7324)	20.9	(8.3)	(0.40)	—	—	—	(7.5)	36	—	—	
25	(NSM.PM 7325)	14.3	5.5	0.38	(3.4)	(0.24)	(0.62)	4.9	34	17	38	
26	(NSM.PM 7326)	(12.7)	4.6	(0.36)	—	—	—	4.0	(31)	—	—	

Table 4. Continued

Specimen	D	H	H/D	B	B/D	B/H	U	U/D (%)	UT	VT	Type*
27 (NSM.PM 7327)	(28.0)	11.8	(0.42)	7.5	(0.27)	0.64	9.6	(34)	(13)	(16×2?)	
28 (NSM.PM 7328)	18.6	6.9	0.37	(4.5)	(0.24)	(0.65)	(7.0)	(38)	—	—	
29 (NSM.PM 7329)	—	(6.8)	—	(4.4)	—	(0.65)	—	—	—	—	
30 (NSM.PM 7330)	(28.0)	(9.7)	(0.35)	—	—	—	11.1	(40)	16	31	C
3F27-1 (NSM.PM 7331)	21.0	9.7	0.46	6.0	0.29	0.62	6.2	30	11	31	
2 (NSM.PM 7332)	16.7	6.7	0.40	(3.3)	(0.20)	(0.49)	5.2	31	(6×2)	(14×2)	
3 (NSM.PM 7333)	(50.4)	18.9	(0.38)	(6.2)	(0.12)	(0.33)	(15.0)	(30)	—	—	B
4 (NSM.PM 7334)	—	—	—	—	—	—	—	—	16	28	B
3F29-1 (NSM.PM 7335)	(52.9)	19.2	(0.36)	14.0	(0.26)	0.73	(17.5)	(33)	(7×2)	(13×2)	C
2 (NSM.PM 7336)	43.9	17.6	0.40	11.1	0.25	0.63	11.5	29	18	(43)	B
3 (NSM.PM 7337)	(33.6)	14.2	(0.42)	8.6	(0.26)	0.61	(10.0)	(30)	12	30	
4 (NSM.PM 7338)	(19.3)	(12.0)	(0.62)	(6.2)	(0.32)	(0.52)	(8.0)	(41)	12	28	
5 (NSM.PM 7339)	(26.2)	11.0	(0.42)	(6.4)	(0.24)	(0.58)	(7.0)	(27)	(10×2)	(14×2)	
6 (NSM.PM 7440)	(22.6)	8.2	(0.36)	6.3	(0.28)	0.77	(6.2)	(27)	13	30	
7 (NSM.PM 7441)	19.9	8.8	0.44	4.6	0.23	0.52	6.3	27	(6×2)	(19×2)	
8 (NSM.PM 7442)	13.5	4.1	0.30	3.1	0.23	0.76	5.7	42	(10×2)	(18×2)	
9 (NSM.PM 7443)	16.9	6.4	0.38	4.1	0.34	0.64	5.8	34	(6×2)	(14×2)	
3002-1 (NSM.PM 7387)	22.2	10.1	0.45	5.1	0.23	0.50	6.2	28	19	51	
2 (NSM.PM 7388)	22.0	9.4	0.43	5.5	0.25	0.59	5.9	27	(10×2)	(19×2)	
3 (NSM.PM 7389)	15.6	6.6	0.42	4.5	0.29	0.68	4.7	30	(8×2)	(19×2)	
4 (NSM.PM 7390)	16.9	7.4	0.44	4.1	0.24	0.55	4.6	27	17	(48)	
5 (NSM.PM 7391)	15.4	6.4	0.42	—	—	—	5.0	32	18	(46)	
6 (NSM.PM 7392)	15.1	6.0	0.40	—	—	—	5.3	35	17	(40)	
7 (NSM.PM 7393)	17.7	7.2	0.41	—	—	—	6.3	36	18	(20×2)	
8 (NSM.PM 7394)	19.1	9.0	0.47	—	—	—	4.9	26	17	46	
9 (NSM.PM 7395)	18.9	5.7	0.30	(3.8)	(0.20)	(0.67)	4.7	25	16	(38)	
10 (NSM.PM 7396)	14.7	5.7	0.39	—	—	—	5.0	34	17	(41)	
11 (NSM.PM 7397)	13.0	4.7	0.36	—	—	—	5.0	38	19	(39)	
12 (NSM.PM 7398)	15.6	6.3	0.40	—	—	—	5.1	33	18	44	
13 (NSM.PM 7399)	14.5	5.9	0.41	(4.0)	(0.28)	(0.68)	4.5	31	13	(36)	
14 (NSM.PM 7400)	13.9	6.5	0.47	(3.3)	(0.24)	(0.51)	3.9	28	—	—	
15 (NSM.PM 7401)	14.1	6.4	0.45	3.4	0.24	0.53	3.8	27	17	46	
16 (NSM.PM 7402)	12.1	3.7	0.31	3.3	0.27	0.89	4.0	33	16	31	
17 (NSM.PM 7403)	14.4	5.7	0.40	—	—	—	4.8	33	16	47	
18 (NSM.PM 7404)	11.8	4.8	0.41	2.8	0.24	0.58	4.0	34	17	(45)	
19 (NSM.PM 7405)	11.4	4.5	0.39	2.8	0.25	0.62	4.0	35	18	(40)	
20 (NSM.PM 7406)	10.9	4.3	0.39	2.8	0.26	0.65	3.8	35	17	(42)	
21 (NSM.PM 7407)	9.1	3.6	0.40	2.6	0.29	0.72	2.8	31	12	—	
22 (NSM.PM 7408)	8.5	3.0	0.35	2.4	0.28	0.80	3.0	35	18	(34)	
23 (NSM.PM 7409)	9.3	3.7	0.40	—	—	—	3.0	32	(15)	(22×2)	
24 (NSM.PM 7410)	10.8	4.6	0.43	2.9	0.27	0.63	3.3	31	(8×2)	(28×2)	
25 (NSM.PM 7411)	9.6	3.6	0.40	2.4	0.25	0.63	3.2	33	(9×2)	(22×2)	
26 (NSM.PM 7412)	10.9	4.7	0.43	3.8	0.35	0.81	2.9	27	(8×2)	—	
27 (NSM.PM 7413)	9.5	3.8	0.40	2.8	0.29	0.74	2.9	31	(15)	(38)	
28 (NSM.PM 7414)	11.5	5.4	0.47	(2.9)	(0.25)	(0.54)	2.9	25	(10×2)	(26×2)	
29 (NSM.PM 7415)	6.7	(2.7)	(0.40)	(2.2)	(0.33)	(0.81)	1.8	27	—	—	

Table 4. Continued

Specimen	D	H	H/D	B	B/D	B/H	U	U/D (%)	UT	VT	Type*
30 (NSM.PM 7416)	9.0	3.0	0.33	2.8	0.31	0.93	3.4	38	(10×2)	(22×2)	
31 (NSM.PM 7417)	7.1	2.7	0.38	2.1	0.30	0.78	2.1	30	(9×2)	(17×2)	
32 (NSM.PM 7418)	22.5	10.4	0.46	—	—	—	6.5	29	16	(39)	
33 (NSM.PM 7419)	24.3	11.6	0.48	5.8	0.24	0.50	5.6	23	17	46	
34 (NSM.PM 7420)	19.4	7.8	0.40	—	—	—	6.2	32	18	(45)	
35 (NSM.PM 7421)	17.0	6.8	0.40	4.2	0.25	0.62	5.7	34	18	—	
36 (NSM.PM 7422)	15.9	7.6	0.48	3.7	0.23	0.49	3.0	19	—	—	
37 (NSM.PM 7423)	17.5	8.7	0.50	4.6	0.26	0.53	3.7	21	14	47	
38 (NSM.PM 7424)	17.4	7.0	0.40	(3.8)	(0.22)	(0.54)	5.7	33	17	(42)	
39 (NSM.PM 7425)	19.2	(8.4)	(0.44)	—	—	—	5.2	27	—	—	
40 (NSM.PM 7426)	14.5	5.6	0.39	3.8	0.26	0.68	5.5	38	18	38	
41 (NSM.PM 7427)	13.3	(6.0)	(0.45)	(2.9)	(0.22)	(0.48)	3.9	29	(8×2)	(24×2)	
42 (NSM.PM 7428)	14.9	6.5	0.44	—	—	—	(3.9)	(26)	(8×2)	(19×2)	
43 (NSM.PM 7429)	13.6	(6.4)	(0.47)	(3.0)	(0.22)	(0.47)	(3.5)	(26)	16	(41)	
44 (NSM.PM 7430)	13.8	5.2	0.38	3.8	0.28	0.73	4.9	36	—	—	
45 (NSM.PM 7431)	13.8	5.8	0.42	3.7	0.27	0.64	4.4	32	(9×2)	(25×2)	
46 (NSM.PM 7432)	13.4	5.5	0.41	—	—	—	3.1	23	(9×2)	(22×2)	
47 (NSM.PM 7433)	12.4	4.8	0.39	3.0	0.24	0.63	4.3	35	20	48	
48 (NSM.PM 7434)	11.9	4.9	0.41	—	—	—	3.8	32	19	(39)	
49 (NSM.PM 7435)	9.1	3.6	0.40	2.2	0.24	0.61	3.1	34	(16)	(38)	
50 (NSM.PM 7436)	10.8	4.7	0.44	3.0	0.28	0.64	3.4	31	16	—	
51 (NSM.PM 7437)	8.7	3.5	0.40	2.2	0.25	0.63	2.2	33	(10×2)	(23×2)	
52 (NSM.PM 7438)	7.7	2.9	0.38	2.0	0.26	0.69	2.6	34	—	—	
53 (NSM.PM 7439)	14.7	4.9	0.33	3.2	0.22	0.65	5.8	39	19	44	
54 (NSM.PM 7476)	22.8	9.5	0.42	6.6	0.29	0.69	7.5	33	19	33	C

* Most specimens, except otherwise noted, are representatives of Type A.

strongly influenced by intervals of data. In this study, we calculated the reduced major axis for the growth of the above-mentioned characters on the assumption of monophasic allometry. The results of average relative growth analysis are summarized as follows.

U to D

Sample	Reduced major axis	r	N	O. R. (Dmm)
PM 3F26	$U=0.346D^{0.994}$	0.9596	30	12.7–39.1
PM 3F29	$U=0.537D^{0.840}$	0.9234	9	13.5–52.9
PM 3002	$U=0.305D^{1.003}$	0.8736	54	7.1–24.3

H to D

Sample	Reduced major axis	r	N	O. R. (Dmm)
PM 3F26	$H=0.280D^{1.104}$	0.9790	30	12.7–39.1
PM 3F29	$H=0.299D^{1.095}$	0.9185	9	13.5–52.9
PM 3002	$H=0.270D^{1.159}$	0.9623	54	7.1–24.3

B to D

Sample	Reduced major axis	r	N	O. R. (Dmm)
PM 3F26	$B=0.099D^{1.286}$	0.9165	23	13.8–39.1
PM 3F29	$B=0.210D^{1.062}$	0.9765	9	13.5–52.9
PM 3002	$B=0.347D^{0.883}$	0.9339	39	7.1–24.3

B to H

Sample	Reduced major axis	r	N	O. R. (Bmm)
PM 3F26	$B=0.505H^{1.091}$	0.9652	24	2.0–10.8
PM 3F29	$B=0.849H^{0.969}$	0.9540	9	3.1–14.0
PM 3002	$B=0.937H^{0.763}$	0.9009	39	2.1– 6.6

As shown in Fig. 8, the samples examined are composed of variously sized specimens; however, a significant correlation coefficient is recognized in the reduced major axis calculated. The slope of the reduced major axis for the growth of umbilical diameter to shell diameter in these samples indicates slight negative allometry, whereas that for the growth of whorl height may be slightly positive allometric or isometric in relation to shell diameter.

Let us compare the above-mentioned results with the data of individual relative growth analysis. The results of average relative growth analysis are almost harmonious with those of individual relative growth analysis (*see* Fig. 5 and Table 3). However, the growth pattern of whorl breadth to diameter in the shells of more than 15 mm in diameter in samples 3F26 and 3F29 is isometric or slightly positive allometric, and the slope of calculated allometric equations is much larger than that in the early to middle growth phases of the present species at less than 10 mm in diameter in the sample PM 3002. In all probability, a critical point exists during the fifth to the sixth whorl for the growth of this character.

Variation

Next, we describe the interspecific variation of the present species from the examination of specimens of a range of sizes in several samples from the Manji area (for the measurements *see* Table 4).

1. Variation in different size-classes

The variation in numbers of umbilical and upper ventrolateral tubercles per whorl, ratio of whorl breadth to whorl height (B/H) and that of umbilicus to shell diameter

Fig. 8. Double logarithmic scatter-diagrams showing the average relative growth of whorl-height and breadth, and umbilical diameter in relation to shell-diameter or whorl-height in samples PM 3002 and PM 3F26. The calculated reduced major axis is shown in each diagram. For abbreviations in this figure see the explanations in the text.

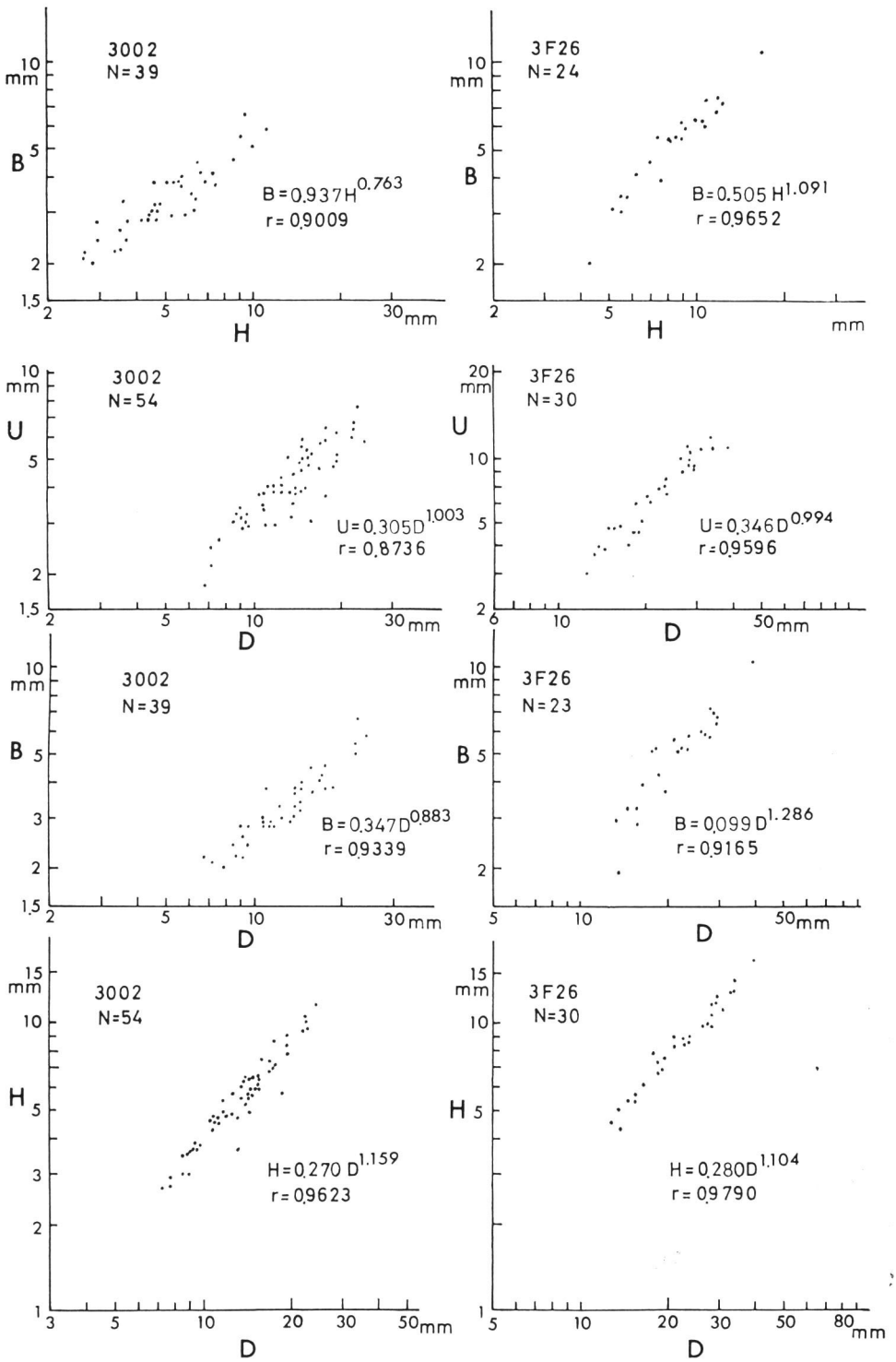
3002
N=39
B=0.937H^0.763
r=0.9009
B
H
mm
3F26
N=24
B=0.505 H^1.091
r=0.9652
3002
N=54
U=0.305D^1.003
r=0.8736
U
D
3F26
N=30
U=0.346D^0.994
r=0.9596
3002
N=39
B=0.347D^0.883
r=0.9339
3F26
N=23
B=0.099D^1.286
r=0.9165
3002
N=54
H=0.270 D^1.159
r=0.9623
H
3F26
N=30
H=0.280D^1.104
r=0.9790

Table 5. Variation of some shell-characters in sample PM 3F26.

Character	Growth stage	D=10–15 mm	D=15–20 mm	D=20–25 mm	D=25–30 mm	D=30–35 mm	D=35–40 mm
Number of umbilical tubercles per whorl	N	1	5	3	8	2	1
	$\bar{X}$	17	14.00	14.67	15.38	18.00	10
	V		11.29	15.75	13.85	7.83	
	s		1.58	2.31	2.13	1.41	
Number of ventro-lateral tubercles per whorl	N	1	4	3	7	2	1
	$\bar{X}$	38	33.50	33.67	37.00	39.50	26
	V		9.28	10.42	18.65	1.80	
	s		3.11	3.51	6.90	0.71	
Ratio of whorl breadth to whorl height	N	3	7	4	7	0	1
	$\bar{X}$	0.57	0.63	0.65	0.61		0.64
	V	14.04	12.70	4.62	6.56		
	s	0.08	0.08	0.03	0.04		
Ratio of umbilicus to shell diameter	N	4	8	6	8	3	1
	$\bar{X}$	0.34	0.34	0.35	0.35	0.34	0.27
	V	5.88	11.76	5.71	8.57	2.94	
	s	0.02	0.34	0.02	0.03	0.01	

Table 6. Variation of some shell-characters in sample PM 3002.

Character	Growth stage	D=5–10 mm	D=10–15 mm	D=15–20 mm	D=20–25 mm
Number of umbilical tubercles per whorl	N	5	15	11	4
	$\bar{X}$	15.20	17.20	17.09	17.75
	V	14.26	10.12	7.14	8.45
	s	2.17	1.74	1.22	1.50
Number of ventro-lateral tubercles per whorl	N	3	14	9	4
	$\bar{X}$	36.67	41.21	44.00	42.25
	V	6.30	11.23	7.62	18.67
	s	2.31	4.63	3.35	7.89
Ratio of whorl breadth to whorl height	N	10	18	7	4
	$\bar{X}$	0.73	0.63	0.58	0.57
	V	13.61	17.46	12.67	15.89
	s	0.10	0.11	0.07	0.09
Ratio of umbilicus to shell diameter	N	11	24	14	5
	$\bar{X}$	0.33	0.32	0.29	0.28
	V	9.09	12.50	17.24	14.29
	s	0.03	0.04	0.05	0.04

(U/D) has been examined in several size-classes in the samples PM 3F26 and PM 3002. The results are summarized in Tables 5–6.

The ratio U/D ranges from 0.19 to 0.41 in specimens of more than 15 mm in shell diameter. Its range of variation in each size-class is usually larger than those in the specimens at 7 to 10 π growth stages (Fig. 5).

The shells with a diameter over 15 mm have a constant form-ratio (B/H) ranging from 0.5 to 0.8, which is much smaller than those in the early growth phase of less than 5 mm in shell diameter.

As compared with the two parameters mentioned above in connection with shell form, the present species shows considerable variation in the number of ventrolateral tubercles per whorl in the shells over 15 mm in diameter.

The number of umbilical tubercles per whorl on the fifth to the seventh whorl ranges from 12 to 19, similar to those on the fourth one.

MATSUMOTO (1959, p. 113) gave measurements on 14 specimens of *S. neptuni* from the Turonian of California. Although the Californian specimens were collected at several localities, they are represented by more or less large specimens (D=25–109 mm). Based on MATSUMOTO's data, let us compare the variation in the Californian specimens with that in the Manji specimens.

The former specimens have the form-ratios B/H and U/D respectively ranging from 0.57 to 0.8 and from 0.25 to 0.31. The range of variation of these two parameters in the Californian specimens is similar to that in the large specimens from the Manji area; thus any significant geographic variation of shell-form is not found between the Manji and Californian specimens.

2. Morphotypic variation

We have distinguished the following morphotypic variation in the specimens of *S. neptuni* from the Upper Turonian of the Manji area, though the morphotypes may grade into one another. We do not intend to give names to these variants which may correspond in part, if not wholly, to what MATSUMOTO (1965, p. 52) mentioned as variants in his description of the Japanese specimens.

The representative specimens of morphotypes A, B, and C are illustrated in Figs. 9~12.

A-1 type: A group of considerable abundance, typically represented by specimen NSM. PM 7051 (Fig. 9–2; Pl. 4, fig. 3) from loc. PM 3F17, in which the umbilicus is quite narrow, the whorl is much compressed, the ribs are rather weak, and the lower ventrolateral tubercles become gradually weaker at about 60 mm diameter.

A-2 type: A group of considerable abundance, typically represented by specimen NSM. PM 7047 (Fig. 9–1; Pl. 4, fig. 2) from loc. PM 3F16, in which the umbilicus is wider, the whorl is less high, and the ribs are stronger in comparison with A-1 type. Double ventrolateral tubercles are also stronger than those of A-1. Thus, group A-2 approaches group C (described below) at about 60 mm diameter. The keel is low, and sometimes has a tubercle-like elevation on the mid-venter at the junction of the ribs.

A-3 type: A group of considerable abundance, typically represented by specimen

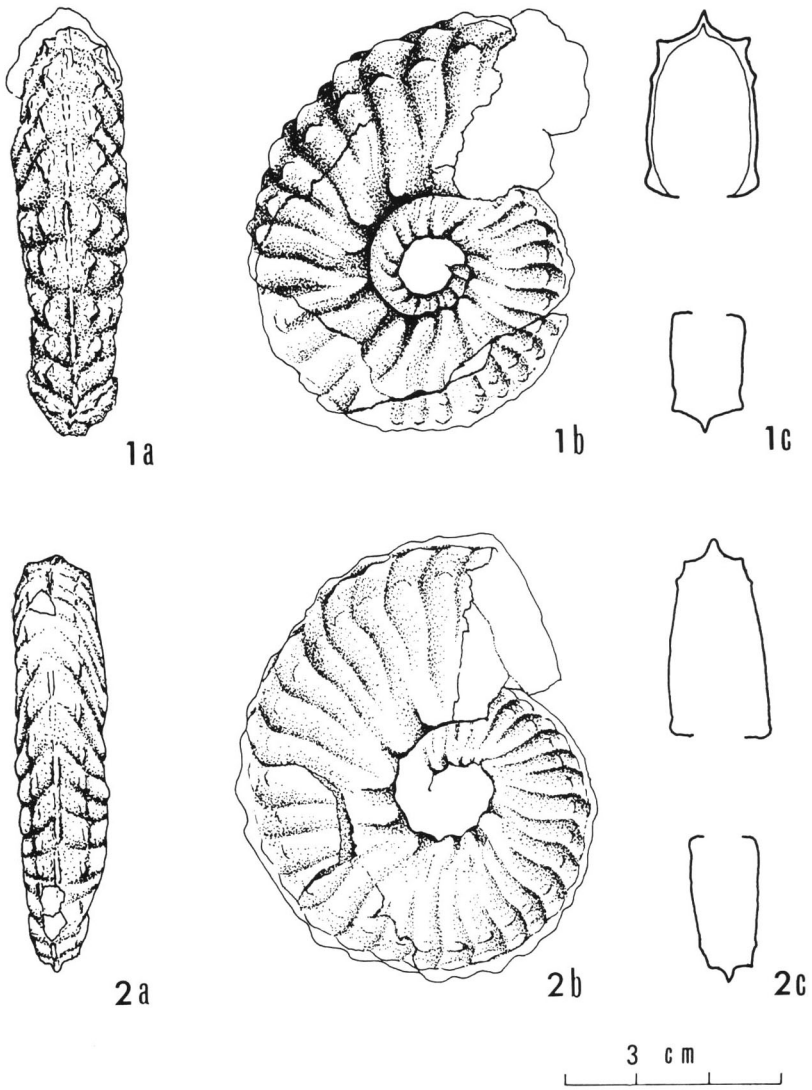

Fig. 9. Drawings showing the morphotypic variation in *S. neptuni*. The characteristic mode of ribbing and tuberculation, and whorl sectional shape are indicated for each morphotype. 1. NSM.PM 7047. Ventral (a), lateral (b) views and diagrammatic whorl section (c). 2. NSM.PM 7051. Ventral (a), lateral (b) views and diagrammatic whorl section (c).

NSM. PM 7301 (Fig. 11–2) from loc. PM 3F26, in which the umbilicus is quite narrow, the whorl is high, convergent and widest at the umbilical margin. Around 30 to 45 mm diameter, the ribs are strong, but the double ventrolateral tubercles decrease in strength. Finally the lower ventrolateral tubercles disappear. The keel is well

developed.

A-4 type: A group of considerable abundance, typically represented by specimen NSM. PM 7303 (Fig. 10–2; Pl. 3, fig. 2) from loc. PM 3F26, in which the ornament is similar to that of the previous three morphotypes, but gradually weakens around 25 to 30 mm diameter. Thus, group A-4 approaches morphotypic group B (described below).

A-5 type: A group of considerable abundance. The typical example is specimen NSM. PM 7311 (Fig. 10–1) from loc. PM 3F26, which closely resembles A-4. The whorl is higher and the upper ventrolateral tubercles stronger than those of the latter. As in the case of morphotype A-4, the lower ventrolateral tubercles become weaker and finally disappear at about 25 to 30 mm diameter. The keel is stronger than that of A-4.

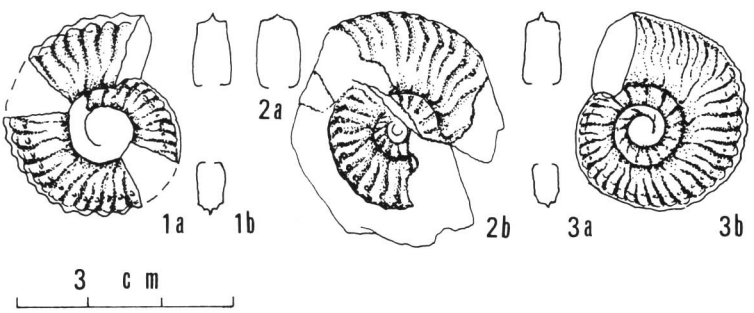

Fig. 10. 1. NSM.PM 7311. Lateral (a) view and diagrammatic whorl section (b). 2. NSM.PM 7303. Diagrammatic whorl section (a) and lateral (b) view. 3. NSM.PM 7302. Diagrammatic whorl section (a) and lateral (b) view.

B-1 type: Rare examples, represented by specimen NSM. PM 7334 (Fig. 11–1) from loc. PM 3F27, in which the umbilicus is moderate in diameter. Below 30 mm diameter, the ribs are strong and double ventrolateral tubercles exist. The lower ventrolateral tubercles gradually decrease in strength with growth, and finally disappear on the weakened ribs around 30 to 45 mm diameter. The upper ventrolateral tubercles become weaker and disappear near the apertural margin. The serrated keel is gradually weakened and becomes smooth.

B-2 type: Rare examples, represented by specimen NSM. PM 7336 (Fig. 11–5; Pl. 3, fig. 7) from loc. PM 3F29, in which the umbilicus is fairly narrow, the form-ratio, B/H, is about 0.6 and the ribs gradually weaken. The lower ventrolateral tubercles weaken and finally disappear at about 30 mm diameter. At the same stage, the upper ventrolateral tubercles and the keel also weaken. Near the apertural margin, the keel seems to become discontinuous and to form tubercle-like elevations.

B-3 type: Rare examples, represented by specimen NSM. PM 7302 (Fig. 10–3) from loc. PM 3F26, in which the umbilicus is moderate in diameter, and the whorls are

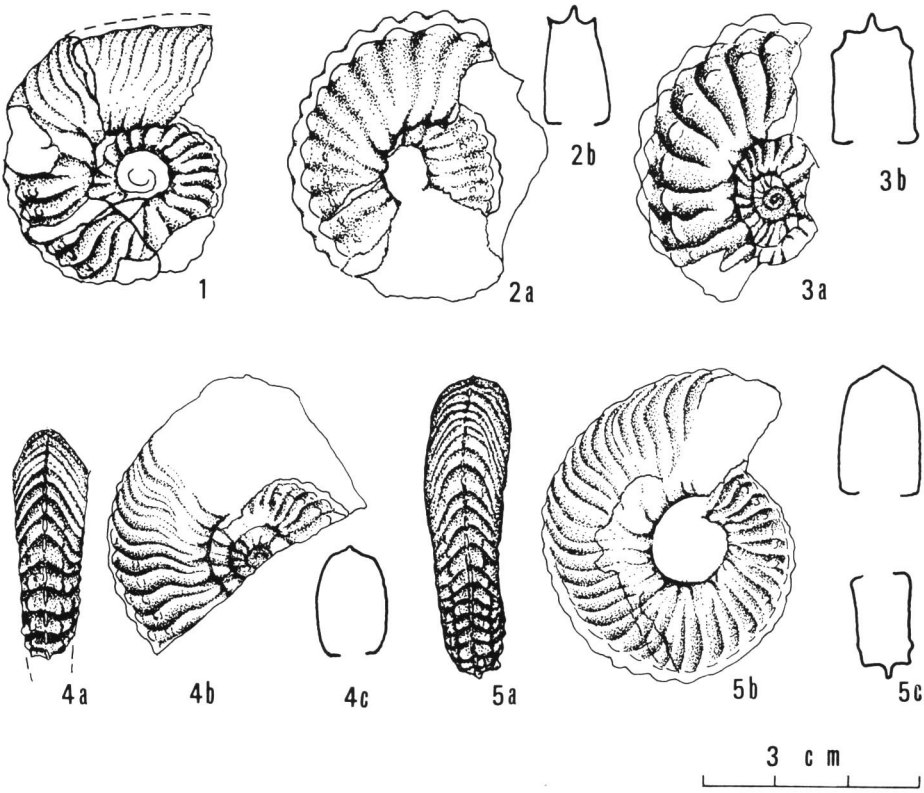

Fig. 11. 1. NSM.PM 7334. Lateral view. 2. NSM.PM 7301. Lateral (a) view and diagrammatic whorl section (b). 3. NSM.PM 7053. Lateral (a) view and diagrammatic whorl section (b). 4. NSM.PM 7344. Ventral (a), lateral (b) views and diagrammatic whorl section (c). 5. NSM.PM 7336. Ventral (a), lateral (b) views and diagrammatic whorl section (c).

inflated and broadest near the umbilical margin. At about 23 mm diameter the ribs, the double ventrolateral tubercles and the umbilical tubercles weaken or disappear. B-3 morphotype represents an intermediate type between A and B.

C type: A fairly abundant group, typically represented by specimens NSM. PM7000 (Fig. 12; Pl. 4, fig. 1) from loc. PM 3F16 and NSM. PM 7053 (Fig. 11–3; Pl. 3, fig. 3) from loc. F1. In the former specimen the umbilicus is wider than those of groups A-1 and A-2, and the umbilical shoulder is angular. The whorl is broader, being subrectangular in cross section, than that of A-2. The ribs are coarser than in other types, gradually getting far apart, and are stronger than those in A-1 and A-2. The double ventrolateral tubercles are strong throughout life. The serrated keel is high and strong. In NSM. PM 7053, the umbilical size is similar to those in morphotypes A-3, B-1 and B-2, and the umbilical shoulder is angular. The ribs are wide apart. The double ventrolateral tubercles are strong. The keel is

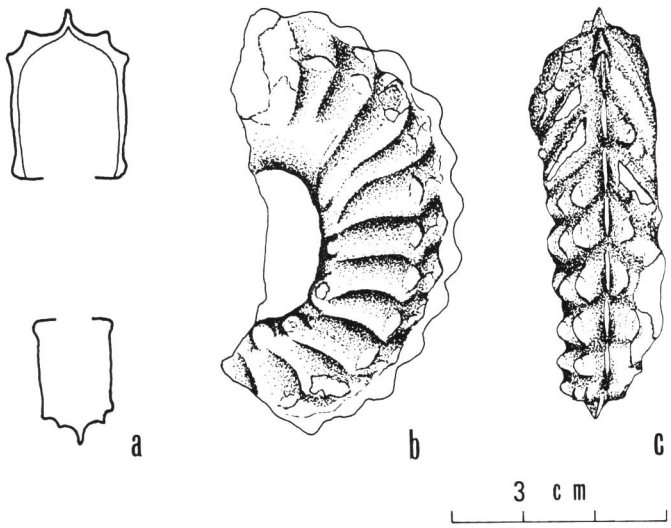

Fig. 12. NSM.PM 7000. Diagrammatic whorl section (a), lateral (b) and ventral (c) views.

distinctly serrated, and is stronger than any of B-1, B-2 and A-3. Thus, morphotype group C approaches the Californian species, *Subprionocyclus branneri* (ANDERSON) (*see* MATSUMOTO, 1959, p. 109, text-figs. 58–59), in morphologic character.

The variation in the surface ornamentation of the young stages of the present species, as described above is very interesting in that it shows affinities to certain other species of the Collignoniceratidae. Group A may be regarded as representing the most typical *S. neptuni*. Group C resembles *S. branneri*, although it has a thinner whorl than the latter. The specimens of group B are always below ca. 30 to 45 mm in diameter, and at about 30 mm the ribs lose their double ventrolateral tubercles and are closely arranged near the apertural margin. Group B could be interpretated as the sexual dimorph of group A, but both groups have intermediate specimens, as represented by those of A-4 and B-3.

The morphotypes described above have similar suture lines to one another, represented by E L U_2 U_3 (=S) U_1 I (*see* Fig. 13).

Ontogenetic Comparison with *S. normalis* and *R. minimus*

MATSUMOTO (1959, 1965) and OBATA (1965) studied the early to middle ontogeny of *S. normalis* and *R. minimus*, and gave systematic descriptions of ontogenetic variation of many characters. According to them, both *S. normalis* and *R. minimus* are very closely allied to *S. neptuni*.

We now compare the ontogenetic development of *S. neptuni* with those of *S. normalis* and *R. minimus* from results of this work and that of MATSUMOTO (1959,

1965) and OBATA (1964, 1965).

1. Comparison of the early growth stage up to 15 mm diameter.

The ontogenetic growth of the suture line and shell form below 15 mm diameter in *S. neptuni*, *R. minimus*, and *S. normalis* is similar in all three species.

Protoconch: The width of the protoconch of *S. neptuni* along the median line is much larger than in *R. minimus* (ca. 0.40 mm by OBATA, 1965). In *R. minimus*, the protoconch is not exposed, being completely enveloped by the first whorl (OBATA, 1965), while it is partly exposed in *S. neptuni* and *S. normalis* (MATSUMOTO, 1965).

The first and the second whorl: Many of the characters in *S. neptuni* show a similar variation to those in *R. minimus*, and no significant difference was observed between the two species.

The third and the fourth whorl: The shell-form ratios U/D and B/H gradually decrease with growth in *S. neptuni, S. normalis* and *R. minimus*. The histograms of characters examined at several growth stages in this phase for these three species are similar to one another.

The fifth whorl: The shell-form ratios, U/D and B/H in *S. neptuni* gradually decrease with growth, similar to *S. normalis* and *R. minimus*. The ontogenetic decrease of U/D in the latter two species is, however, more rapid than the former. As compared with *S. neptuni, R. minimus* has a considerable range of variation for the number of umbilical and ventrolateral tubercles per whorl in this stage. Up to 15 mm in diameter, the growth pattern of whorl height and breadth, and umbilical diameter in relation to shell diameter or whorl height in *S. neptuni* and *R. minimus* resemble each other.

2. Comparison of the middle growth stage beyond 15 mm diameter

At larger sizes the form ratio U/D in *R. minimus* gradually decreases with growth, while *S. normalis* and *S. neptuni* do not show any significant ontogenetic change for this character. The significant differences among the three species at this stage may be the mode of tuberculation and ribbing.

The number of umbilical tubercles per whorl in this stage of *S. neptuni* ranges from 10 to 20, being somewhat more numerous than in *R. minimus* and *S. normalis* (*see* OBATA, 1965, text-fig. 25).

According to OBATA (1965, text-fig. 25), *S. normalis* has about 15 to 30 ventrolateral tubercles per whorl on the sixth to the eighth whorls, being less numerous than those in *S. neptuni* which bears more than 30.

The details of tuberculation and ribbing in the middle to later stages of these

Fig. 13. Sutural patterns in selected specimens of *S. neptuni*.
A: Sutural variation demonstrated by selected examples;
(1): NSM.PM 7387, (2): NSM.PM 7476, (3): NSM.PM 9249, (4): NSM.PM 9248, (5): NSM.PM 7423, (6): NSM.PM 7431, (7): NSM.PM 7428, (8): NSM.PM 7430, (9): NSM.PM 7319, (10): NSM.PM 7438, (11): NSM.PM 7321.
B: Ontogenetic change in early growth stage of NSM.PM 7401.

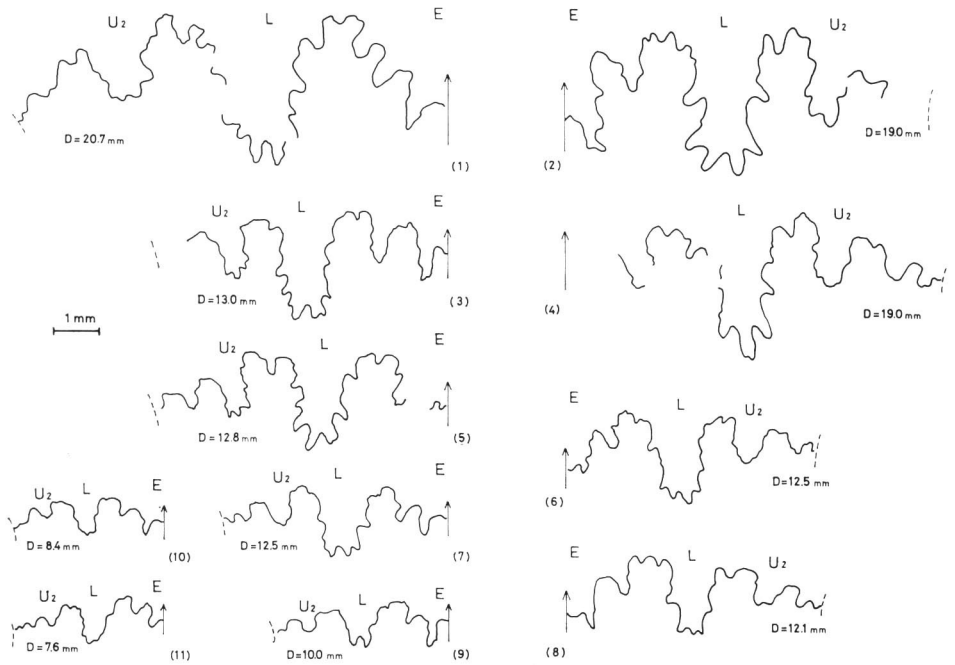
U2
L
E
D = 20.7 mm
(1)
E
L
U2
D = 19.0 mm
(2)
U2
L
E
D = 13.0 mm
(3)
1 mm
L
U2
(4)
D = 19.0 mm
U2
L
E
D = 12.8 mm
(5)
E
L
U2
D = 12.5 mm
(6)
U2
L
E
D = 8.4 mm
(10)
U2
L
E
D = 12.5 mm
(7)
E
L
U2
D = 12.1 mm
(8)
U2
L
E
D = 7.6 mm
(11)
U2
L
E
D = 10.0 mm
(9)

A

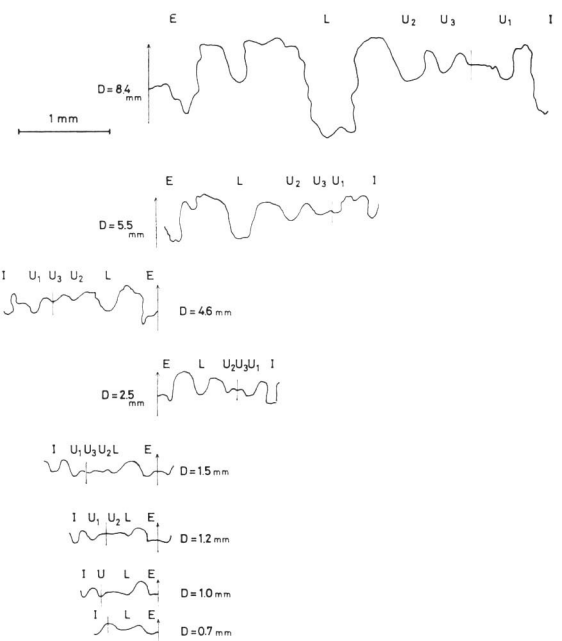
E
L
U2
U3
U1
I
D = 8.4 mm
1 mm
E
L
U2 U3 U1
I
D = 5.5 mm
I
U1 U3 U2
L
E
D = 4.6 mm
E
L
U2U3U1
I
D = 2.5 mm
I U1U3U2L
E
D = 1.5 mm
I U1 U2 L
E
D = 1.2 mm
I U L
E
D = 1.0 mm
I
L
E
D = 0.7 mm

B

three species are described in the next chapter.

Allometric Evolution

As MATSUMOTO (1959, 1965) and OBATA (1965) have already mentioned, *S. neptuni*, *S. normalis* and *R. minimus* may have evolved from a common ancestor.

OBATA (1965) examined the interspecific relationship among these three species from the viewpoint of phylogenetic allometry. According to OBATA, the line of phylogenetic allometries of several shell characters in these species corresponds with the lines of ontogenetic allometry of *S. neptuni*; thus the corresponding line of phylogenetic allometry is controlled by the shell size and the slope of relative growth of *S. neptuni* among the three species.

Recently, REYMENT (1975) tried to demonstrate the patterns of evolution in the "*S. neptuni-S. normalis-R. minimus* lineage" from the multivariate morphometrical treatment of several population samples of these three species.

He concluded that the patterns of evolution in the above-mentioned "lineage" may be discontinuous, as explained by the model of punctuated equilibria (ELDREDGE and GOULD, 1972).

REYMENT's data are, however, based on the measurements of variously sized shells, and he did not consider the ontogenetic variation of shell characters.

As already described in this paper and others (*e.g.* MATSUMOTO, 1965, OBATA, 1965), *S. neptuni, S. normalis* and *R. minimus* all display considerable variation for many characters in the early to middle growth stages. Therefore, we should take the ontogenetic variation into consideration to determine the patterns of evolution of these species.

To investigate the patterns of evolution in the Turonian collignoniceratids in connection with the "*S. neptuni-S. normalis-R. minimus* lineage", we have further examined the interspecific variation in the different size-classes and average relative growth in such species as *Collignoniceras woollgari, Subprionocyclus bravaisianus, S. normalis, R. minimus* and *R. elegans*, all of which are closely allied to *S. neptuni*. The locality guide and repository of the samples of these species examined have already been given.

The calculated reduced major axis showing the average relative growth of umbilicus, whorl height and breadth in relation to shell diameter or whorl height in these species is summarized in Table 7. The data of average relative growth in *S. neptuni* have already shown on p. 67–68.

As given in Table 7, high degrees of correlation are recognized in most of the calculated allometric equations, except for the growth of umbilicus to diameter in the three samples (SN 2F01, RN 8001 and SN 2003) of *R. minimus*. Therefore, the growth pattern of the other characters in the specimens so far examined in such species as *C. woollgari, S. bravaisianus, S. neptuni, S. normalis* and *R. elegans* may be regarded as monophasic allometry. The growth of whorl-height and breadth to

Table 7. Average relative growth for several characters in selected Turonian collignoniceratid species.

(U to D)

Species	Sample	Reduced major axis	r	N	O. R. of D mm
C. woollgari	OB	$U=0.359D^{1.034}$	0.9962	24	6.2—33.1
S. bravaisianus	Uchaux	$U=0.369D^{1.014}$	0.9800	11	11.8—60.0
S. normalis	CIT1346	$U=0.546D^{0.754}$	0.8587	13	15.0—44.0
R. minimus	IK 946	$U=0.515D^{0.779}$	0.9328	35	5.3—27.6
〃	IK 938	$U=1.039D^{0.513}$	0.8878	11	8.6—33.3
〃	SN 2F01	$U=0.439D^{0.822}$	0.7946	45	11.0—57.6
〃	RN 8001	$U=0.714D^{0.647}$	0.7686	28	6.9—38.4
〃	SN 2003	$U=0.592D^{0.727}$	0.7818	59	7.8—39.6
R. elegans	Haboro	$U=0.868D^{0.563}$	0.8982	7	8.5—28.5

(H to D)

Species	Sample	Reduced major axis	r	N	O. R. of D mm
C. woollgari	OB	$H=0.370D^{0.972}$	0.9962	24	6.2—33.1
S. bravaisianus	Uchaux	$H=0.501D^{0.899}$	0.9867	11	11.8—60.0
S. normalis	CIT1346	$H=0.299D^{1.138}$	0.9921	13	15.0—44.0
R. minimus	IK 946	$H=0.259D^{1.159}$	0.9870	35	5.3—27.6
〃	IK 938	$H=0.223D^{1.235}$	0.9950	11	8.6—33.3
〃	SN 2F01	$H=0.257D^{1.191}$	0.9772	44	11.0—57.6
〃	RN 8001	$H=0.208D^{1.258}$	0.9894	28	6.9—38.4
〃	SN 2003	$H=0.224D^{1.225}$	0.9728	55	7.8—39.6
R. elegans	Haboro	$H=0.272D^{1.136}$	0.9968	7	8.5—28.5

(B to D)

Species	Sample	Reduced major axis	r	N	O. R. of D mm
C. woollgari	OB	$B=0.420D^{0.864}$	0.9861	24	6.2—33.1
S. bravaisianus	Uchaux	$B=0.573D^{0.726}$	0.8548	5	11.8—20.0
S. normalis	CIT1346	$B=0.281D^{0.988}$	0.9871	13	4.2—12.5
R. minimus	IK 946	$B=0.357D^{0.880}$	0.9854	28	5.3—27.6
〃	IK 938	$B=0.286D^{0.969}$	0.9776	9	10.3—33.3
〃	SN 2F01	$B=0.281D^{0.961}$	0.9815	40	11.0—57.6
〃	RN 8001	$B=0.338D^{0.894}$	0.9883	26	6.9—38.4
〃	SN 2003	$B=0.306D^{0.914}$	0.9745	55	7.8—39.6
R. elegans	Haboro	$B=0.455D^{0.754}$	0.9657	7	8.5—28.5

(B to H)

Species	Sample	Reduced major axis	r	N	O. R. of B mm
C. woollgari	OB	$B=1.012H^{0.897}$	0.9891	25	2.0— 8.5
S. bravaisianus	Uchaux	———	———	5	3.8— 5.0
S. normalis	CIT1346	$B=0.803H^{0.868}$	0.9244	13	4.2—12.5
R. minimus	IK 946	$B=0.969H^{0.746}$	0.9852	36	1.8— 6.6
〃	IK 938	$B=0.998H^{0.740}$	0.9633	14	2.5— 8.8
〃	SN 2F01	$B=0.838H^{0.811}$	0.9725	40	2.9—13.4
〃	RN 8001	$B=1.030H^{0.711}$	0.9875	26	1.9— 8.8
〃	SN 2003	$B=0.932H^{0.746}$	0.9697	55	7.8—39.6
R. elegans	Haboro	$B=1.044H^{0.635}$	0.9681	7	2.4— 6.2

diameter, and that of whorl-breadth to height represent monophasic allometry with a high correlation coefficient. In contrast, the growth of umbilicus to diameter in *R. minimus* may display polyphasic allometry, as OBATA (1965) has already pointed out.

Any significant difference in growth ratio for the growth of whorl-breadth to diameter was not found among the six species examined. However, systematic differences in growth ratios of umbilicus to diameter, and of whorl-breadth to height are recognized among these species.

The slope of the reduced major axis for the growth of the above-mentioned characters progressively decreases from the stratigraphically oldest species (*C. woollgari*) to the youngest one (*R. elegans*); for example, the slope for the growth of umbilicus to diameter decreases gradually from isometry in *C. woollgari* and *S. neptuni* to strong negative allometry (α=ca. 0.5) in *R. elegans*, via slight negative allometry in *S. normalis*.

These results agree with OBATA's (1965) preliminary observation; and both are well demonstrated by the diagram Fig. 14 showing the ontogenetic change of shell-form ratios, B/H and U/D.

If we grant the phylogenetic line from *C. woollgari* to *R. elegans* via *S. bravaisianus, S. neptuni, S. normalis* and *R. minimus*, these Turonian collignoniceratids have evolved to become more narrowly umbilicate and more compressed.

Evolutionary Change of Surface Ornament and Suture

As MATSUMOTO (1965, p. 62) mentioned, *Reesidites* is a derivative of *Subprionocyclus* judging from the morphological resemblance and the stratigraphically successive occurrence, a major distinction being the complete disappearance of the inner ventrolateral tubercles in *Reesidites*. *S. normalis* has a more fastigate venter, weaker ornament and a shorter period of double ventrolateral tubercles than *S. neptuni* (MATSUMOTO, 1959, p. 121). *S. branneri* from the Turonian of California differs from *S. neptuni* in its coarser ornament, the predominance of simple over paired ribs and its more persistent double ventrolateral tubercles, aside from the whorl shape (MATSUMOTO, 1959, p. 111).

The doubling of the ventrolateral tubercles, without showing large horn-like tubercles, and the moderately strong, instead of very coarse, ribbing and the nearly rectangular whorl section are criteria for distinguishing *S. branneri* from *C. woollgari* (MATSUMOTO, 1959, p. 111). The lower ventrolateral tubercles are weakened on the outer whorl of *S. neptuni*, while the double ventrolateral tubercles are united into prominent horns on that of *C. woollgari*.

Fig. 14. Double scatter-diagrams showing the ontogenetic change of the relationship between the ratio of umbilical diameter to shell-diameter (U/D) and that of whorl-breadth to whorl-height (B/H) in selected Turonian collignoniceratids. For abbreviations in this figure see the explanations in the text. See errata on p. 86.

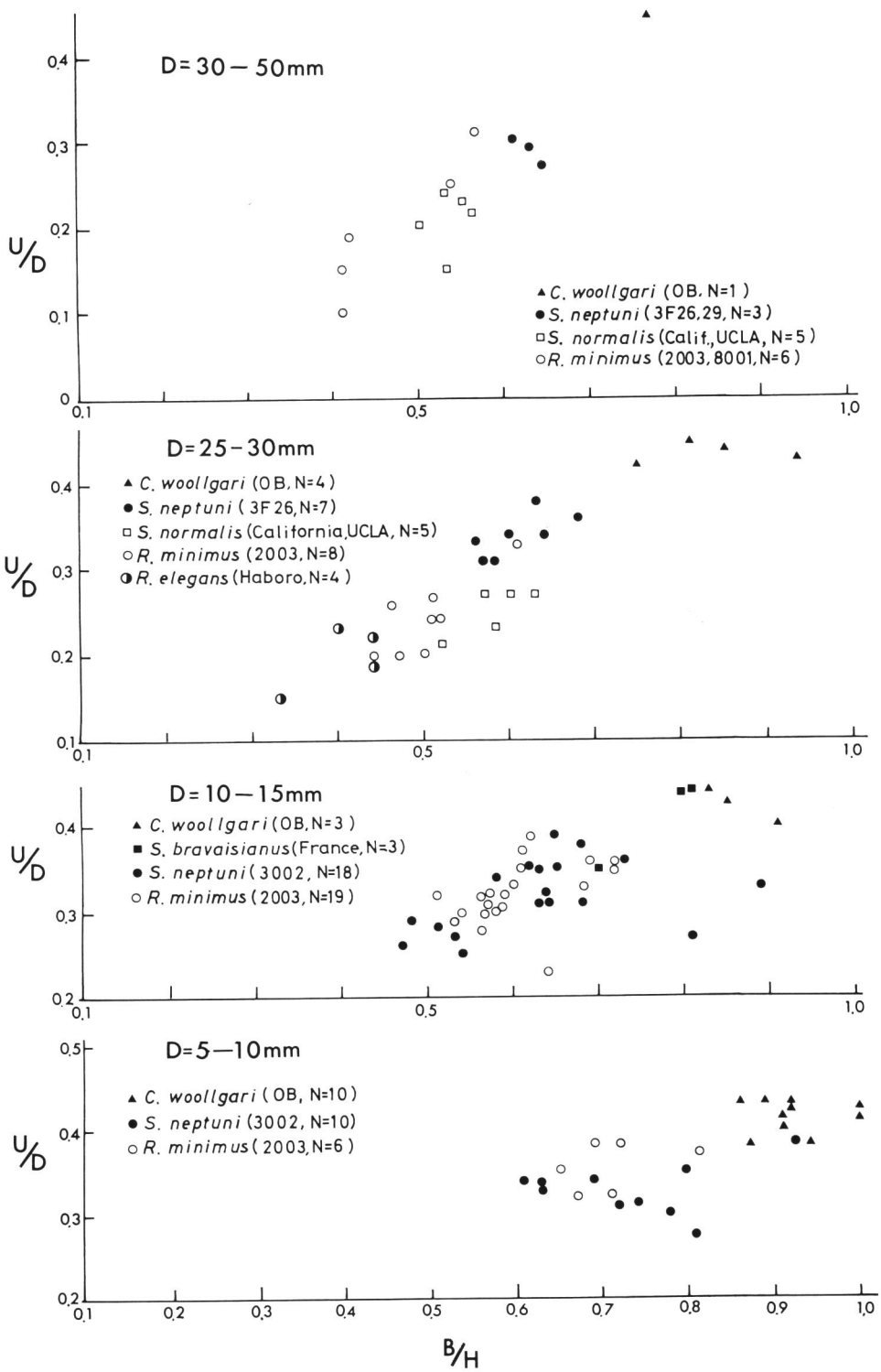
D=30—50mm
▲C. woollgari (OB, N=1)
●S. neptuni (3F26,29, N=3)
□S. normalis (Calif., UCLA, N=5)
○R. minimus (2003, 8001, N=6)
D=25—30mm
▲C. woollgari (OB, N=4)
●S. neptuni (3F26, N=7)
□S. normalis (California, UCLA, N=5)
○R. minimus (2003, N=8)
◑R. elegans (Haboro, N=4)
D=10—15mm
▲C. woollgari (OB, N=3)
■S. bravaisianus (France, N=3)
●S. neptuni (3002, N=18)
○R. minimus (2003, N=19)
D=5—10mm
▲C. woollgari (OB, N=10)
●S. neptuni (3002, N=10)
○R. minimus (2003, N=6)
U/D
B/H

Also on the outer whorl the ribs are much stronger and far apart in *C. woollgari* than in *S. neptuni* (MATSUMOTO, 1959, p. 117).

To sum up, the mode of ribbing and strength of tubercles are weakened along the "phylogenetic line" of *C. woollgari-S. branneri-S. neptuni-S. normalis-R. minimus* in ascending order. Although the degree of development of ventrolateral and umbilical tubercles in these species varies from specimen to specimen or stage by stage, the number of tubercles per whorl tends to decrease along the "phylogenetic line", as represented in Fig. 15.

Recently, CHAMBERLAIN (1971, 1976) and CHAMBERLAIN and WESTERMANN (1976) demonstrated experimentally with actual specimens or simulated models that the ectocochliate cephalopod shells with compressed whorl section, narrower umbilicus and weaker shell ornament are better streamlined than those with depressed whorl section, wider umbilicus and stronger ornament. Hence, the patterns of evolution of shell form and surface ornament in the collignoniceratids may represent an improvement in swimming ability.

The suture line of *Reesidites, Subprionocyclus* and *Collignoniceras* is expressed by the formula, E L U_2 U_3 (=S) U_1 I. In the pattern of sutures, *R. minimus* and *S. normalis* closely resemble each other (MATSUMOTO, 1965, p. 66, 68). Their sutures are generally of the same pattern as that of *S. neptuni*, but their saddles are more slender, their lobes are narrower and deeper, and minor incisions are sharper than in the corresponding growth stage of the latter. The saddle between E and L is very asymmetric (MATSUMOTO, 1959, p. 120). In *S. neptuni* and *S. branneri*, the suture is relatively simple, being incised by small dentations. Lateral lobes are V-shaped in general outline, whereas saddles are massive (MATSUMOTO, 1959, p. 110, 114; 1965, p. 54). In *C. woollgari* the saddles are rather massive, and the minor indentations are rather shallow (MATSUMOTO, 1965, p. 12). Thus, we may conveniently classify the sutural pattern of these species into two groups: *R. minimus-S. normalis*, and *S. neptuni-S. branneri-C. woollgari*. The former group has more slender saddles, narrower and deeper lobes and sharper minor lobe incisions than the latter.

According to TANABE's unpublished data, the slope of the allometric equation for the growth of the outer ventral shell wall and septal thickness in relation to shell diameter in *R. minimus* is less than those in *C. woollgari* and *S. neptuni*. As SEILACHER (1975) and TANABE (1977) have mentioned, the evolution of ammonoid sutures in several stocks (*e.g.* scaphitids) has reduced the unsupported areas in the phragmocone-wall to a minimum, allowing further thinning of the outer wall. The evolutionary pattern of sutures and growth of shell-wall-thickness in the collignoniceratids at species level may well accord with this generalized evolutionary pattern of ammonoid sutures. Judging from the evolutionary pattern of sutures and shell-

Fig. 15. Double scatter-diagrams showing the ontogenetic change of the relationship between the numbers of umbilical (UT) and upper ventrolateral (VT) tubercles per whorl in selected Turonian collignoniceratids. For abbreviations in this figure see the explanations in the text. See errata on p. 86.

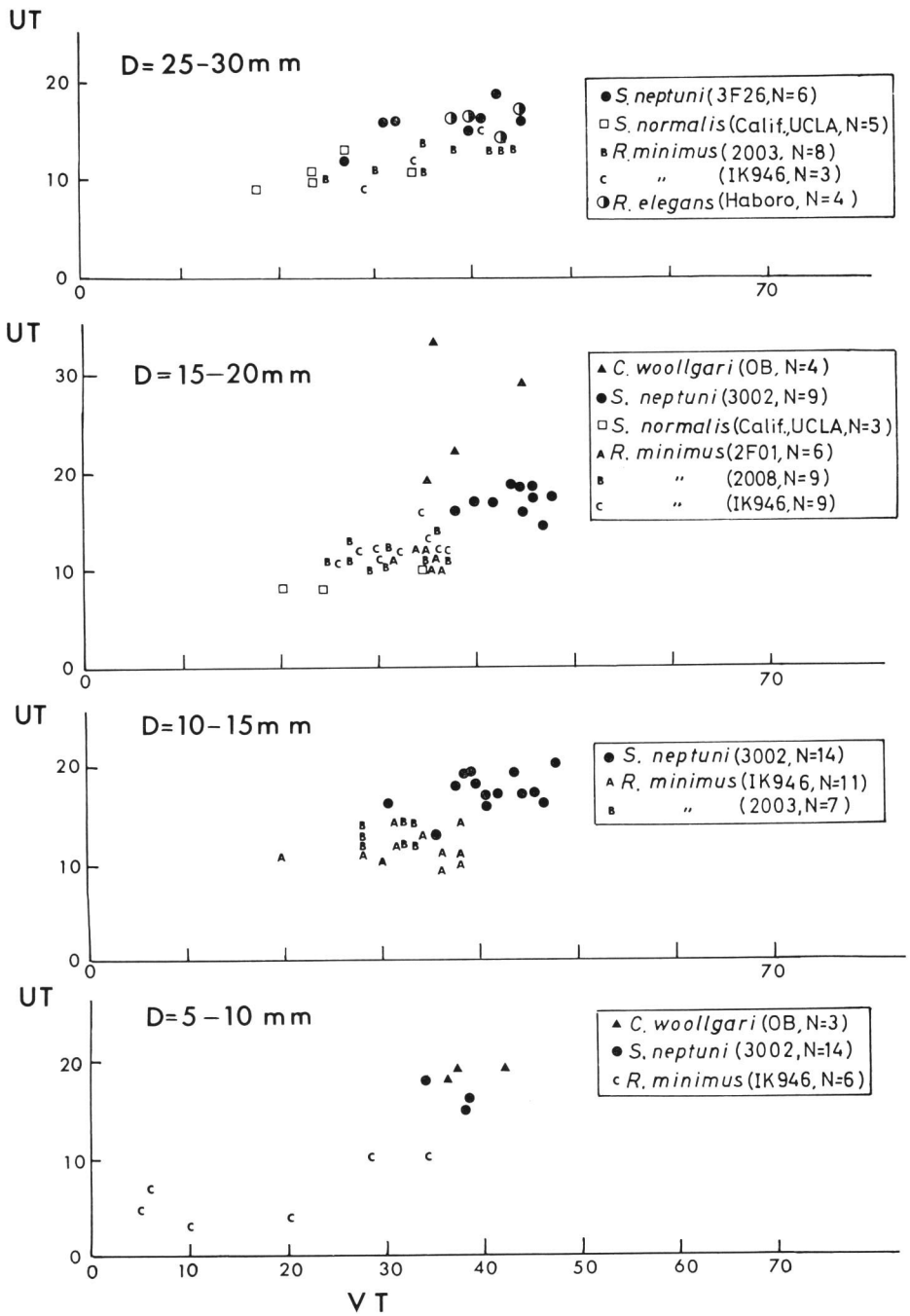
UT
D= 25-30m m
● S. neptuni (3F26, N=6)
□ S. normalis (Calif., UCLA, N=5)
B R. minimus (2003, N=8)
C " (IK946, N=3)
◑ R. elegans (Haboro, N=4)
UT
D=15—20m m
▲ C. woollgari (OB, N=4)
● S. neptuni (3002, N=9)
□ S. normalis (Calif., UCLA, N=3)
A R. minimus (2F01, N=6)
B " (2008, N=9)
C " (IK946, N=9)
UT
D=10-15m m
● S. neptuni (3002, N=14)
A R. minimus (IK946, N=11)
B " (2003, N=7)
UT
D=5-10 mm
▲ C. woollgari (OB, N=3)
● S. neptuni (3002, N=14)
C R. minimus (IK946, N=6)
VT

wall-thickness, the collignoniceratids may have evolved in the direction of an increase in buoyancy.

Finally, we would mention briefly the probable habitats of these collignoniceratids in connection with adaptive evolution. As MATSUMOTO (1960, p. 173) pointed out, ornate ammonoids, such as the collignoniceratids and the acanthoceratids, occur in comparatively shallow water sediments of a marginal shelf facies in California and Oregon. This observation was recently confirmed by us in the Upper Cretaceous of Hokkaido from ammonoid biofacies-analysis in relation to lithofacies (OBATA and FUTAKAMI, 1977; TANABE *et al.*, 1978).

In the Turonian of Hokkaido, *C. woollgari* is commonly found in the silty mudstone to sandy siltstone lithologies of the nearshore to offshore intermediate facies of shallow to moderate depth in the central part of the south western Cretaceous region of Hokkaido, together with many heteromorph ammonoids such as scaphitids, baculitids, nostoceratids and diplomoceratids.

In contrast, both *S. neptuni* and *R. minimus* are restricted to the fine sandstone to silty sandstone lithologies of the inshore to nearshore shallow water facies in the westernmost areas in the south western Cretaceous region of Hokkaido, associated with many drifted plant remains, thick-shelled bivalves and gastropods (OBATA and FUTAKAMI, 1977; TANABE *et al.*, 1978).

Taking all the facts into account, we are inclined to consider that the "phylogenetic line" from *C. woollgari* to *R. minimus* via *S. neptuni* and *S. normalis* probably represents adaptation to shallower sea environments. This fits the evolutionary model of ammonoid habitats proposed by WIEDMANN (1973, fig. 11).

In this study we could not decide whether the patterns of evolution in our collignoniceratids are phyletic gradualism in a single lineage or discontinuous evolution in the sense of punctuated equilibria as used by ELDREDGE and GOULD (1972). However, the field evidence that *S. neptuni* ranges from the Middle Turonian to the upper part of the Upper Turonian in the sequence of Hokkaido, is important to consider the evolutionary pattern in these Turonian collignoniceratids.

Time consuming examination of many population samples of these collignoniceratids from successive stratigraphic levels over a wide area may solve the problem.

Acknowledgements— We are grateful to Professor Emeritus Tatsuro MATSUMOTO of Kyushu University for fruitful discussions and for valuable suggestions. We also appreciate the discussions provided by Drs. J. M. HANCOCK of King's College, London and I. HAYAMI of University of Tokyo. This work was supported partly by the Science Research Fund of the Japanese Ministry of Education, Science and Culture (OBATA, No. 254267 for 1977 and TANABE, No. 374257 for 1978).

References

ANDERSON, F. M., 1958. Upper Cretaceous of the Pacific Coast. *Geol. Soc. Amer., Mem.*, **71**: 378 p., 75 pls.

CHAMBERLAIN, J. A. JUN., 1971. Shell morphology and the dynamics of sreamlining in ectocochliate cephalopods. *Geol. Soc. Amer., Program Ann. Meetings for 1971*: 523–524 (Abstract).

CHAMBERLAIN, J. A. JUN., 1976. Flow patterns and drag coefficients of cephalopod shells. *Palaeontology*, **19**: 539–563, pl. 84.

CHAMBERLAIN, J. A. JUN., & G. E. G. WESTERMANN, 1976. Hydrodynamic properties of cephalopod shell ornament. *Paleobiology*, **2**: 316–331.

COLLIGNON, M., 1931. Faunes sénoniennes du Nord et de l'Ouest de Madagascar. *Ann. géol. Serv. Mines. Madagascar*, **1**: 1–64, pls. 1–9.

ELDREDGE, N. & S. J. GOULD, 1972. Punctuated equilibria: an alternative to phyletic gradualism. *In* T. J. M. SCHOPF (ed.): *Models in Paleobiology*, 82–115. Freeman, Cooper & Co., California.

GEINITZ, H. B., 1849. *Das Quadersandstein oder Kreidegebirge in Deutschland.* 293 p., 12 pls., Freiburg.

HANCOCK, J. M., W. J. KENNEDY & C. W. WRIGHT 1977. Towards a correlation of the Turonian sequences of Japan with those of north-west Europe. *Palaeont. Soc. Japan, Spec. Paps.*, (21): 151–168.

HAYAMI, I. & A. MATSUKUMA, 1970. Variation of bivariate characters from the standpoint of allometry. *Palaeontology*, **13**: 588–605.

HUXLEY, J. S., 1932. *Problems of Relative Growth.* 276 p. Dial Press, New York.

KERMACK, K. A. & J. B. S. HALDNE, 1950. Organic correlation and allometry. *Biometrika*, **37**: 30–41.

MATSUMOTO, T., 1959–60. Upper Cretaceous ammonites of California, Parts II & III. *Mem. Fac. Sci., Kyushu Univ., Ser. D (Geol.)*, Special vol. **1**: 172 p., 41 pls. (Part II), Special vol. **2**: 204 p. (Part III).

MATSUMOTO, T., 1965. A monograph of the Collignoniceratidae from Hokkaido, Part I. *Ibid.*, **16**: 1–80, pls. 1–18.

MATSUMOTO, T. & A. INOMA, 1971. *Reesidites elegans* MATSUMOTO and INOMA, sp. nov. *In* MATSUMOTO, T; A monograph of the Collignoniceratidae from Hokkaido, Part V. *Mem. Fac. Sci., Kyushu Univ., Ser. D (Geol.)*, **21**: 139–142 (129–162), pl. 23, figs. 1–3 (pls.21–24).

MATSUMOTO, T. & M. NODA, 1966. Notes on *Ammonites bravaisianus* D'ORBIGNY from the Cretaceous of France. *Trans. Proc. Palaeont. Soc. Japan, N.S.*, (64): 359–365, pl. 40.

OBATA, I., 1959. Croissance relative sur quelques Espèces des Desmoceratidae. *Mem. Fac. Sci., Kyushu Univ., Ser. D (Geol.)*, **9**: 33–45, pls. 3–5.

OBATA, I., 1960. Spirale de quelques ammonites. *Ibid.*, **9**: 151–163, pl. 15.

OBATA, I. 1964. Notes on ontogeny of *Reesidites minimus*. *Kaseki (Fossils)*, (8): 94–102 (in Japanese).

OBATA, I., 1965. Allometry of *Reesidites minimus*, a Cretaceous ammonite species. *Trans. Proc. Palaeont. Soc. Japan, N.S.*, (58): 39–63, pls. 4–5.

OBATA, I. & M. FUTAKAMI, 1977. The Cretaceous sequence of the Manji dome, Hokkaido. *Palaeont. Soc. Japan, Special Paps.*, (21): 23–30.

PERVINQUIÈRE, L., 1907. Études de paléontologie tunisienne. 1. Céphalopodes des Terrains secondaires. *Carte geol. Tunise*: 428 p., 27 pls.

RAUP, D. M. & A. MICHELSON, 1965. Theoretical morphology of the coiled shells. *Science*, **147**: 1294–1295.

REYMENT, R. A., 1975. Analysis of a generic level transition in Cretaceous ammonites. *Evolution*, **28**: 665–676.

SEILACHER, A., 1975. Mechanische Simulation und funktionelle Evolution des Ammoniten-Septums. *Paläont. Z.*, **49**: 268–286.

TANABE, K., 1977. Functional evolution of *Otoscaphites puerculus* (JIMBO) and *Scaphites planus* (YABE), Upper Cretaceous ammonites. *Mem. Fac. Sci., Kyushu Univ., Ser. D (Geol.)*, **23**: 367–407, pls. 62–64.

TANABE, K., I. OBATA, & M. FUTAKAMI, 1978. Analysis of ammonoid assemblages in the Upper

Turonian of the Manji area, central Hokkaido. *Bull. Natn. Sci. Mus., Ser. C*, **4**: 37–62, pl. 1.

TANABE, K., H. HIRANO, T. MATSUMOTO, and Y. MIYATA, 1977. Stratigraphy of the Upper Cretaceous deposits in the Obira area, northwestern Hokkaido. *Sci. Rep. Dept. Geol. Kyushu Univ.*, **12**: 181–202 (in Japanese with English abstract).

THOMPSON, D'arcy, W., 1917. *On Growth and Form.* 1116 p., Cambridge Univ. Press, London.

WIEDMANN, J., 1973. Evolution or revolution of ammonoids at Mesozoic system boundaries. *Biol. Rev.*, **48**: 159–194.

WOOD, H., 1896. The mollusca of the Chalk Rock, Part I. *Quart. Jour. Geol. Soc. London*, **52**: 69–98, pls. 2–4.

WRIGHT, C. W. & T. MATSUMOTO, 1954. Some doubtful Cretaceous ammonite genera from Japan and Saghalien. *Mem. Fac. Sci., Kyushu Univ., Ser. D (Geol.)*, **4**: 107–134, pls. 7–8.

WRIGHT, C. W. & E. V. WRIGHT, 1951. A survey of the fossil Cephalopoda of the Chalk of Great Britain. Primarily a nomenclatorial revision of Daniel SHARPE's "Description of the fossil remains of mollusca found in the Chalk of England, Part I. Cephalopoda" (1853–1857). *Palaeontgr. Soc.* (1950), 40 p.

Errata of Fig. 14

		Read	For
R. minimus	D=10–15 mm	N=20	N=19

Errata of Fig. 15

		Read	For
R. minimus	D=15–20 mm	2003	2008
S. neptuni	D= 5–10 mm	N= 3	N=14
〃	D=15–20 mm	N=10	N= 9
〃	D=25–30 mm	N= 7	N= 6

Explanation of Plates

Subprionocyclus neptuni (GEINITZ)

All photos, with whitening, by FUTAKAMI.

Plate 1

Fig. 1. Lateral (a, c), frontal (b) and ventral (d) views of NSM.PM 7438 from loc. PM 3002, ×3.
Fig. 2. Lateral (a, c), frontal (b) and ventral (d) views of NSM.PM 7408 from loc. PM 3002, ×3.
Fig. 3. Lateral (a, c), frontal (b) and ventral (d) views of NSM.PM 7426 from loc. PM 3002, ×3.
Fig. 4. Lateral (a, c), frontal (b) and ventral (d) views of NSM.PM 7390 from loc. PM 3002, ×3.
Fig. 5. Lateral (a, c), frontal (b) and ventral (d) views of NSM.PM 7439 from loc. PM 3002, ×3.

Plate 2

Fig. 1. Lateral (a, c), frontal (b) and ventral (d) views of NSM.PM 7388 from loc. PM 3002, ×1.2.
Fig. 2. Lateral (a, c), frontal (b) and ventral (d) views of NSM.PM 7476 from loc. PM 3002, ×1.2.
Fig. 3. Lateral (a, c), frontal (b) and ventral (d) views of NSM.PM 7419 from loc. PM 3002, ×1.2.
Fig. 4. Lateral (a, c), frontal (b) and ventral (d) views of NSM.PM 9249 from loc. PM 3F30, ×1.2.
Fig. 5. Lateral (a, c), frontal (b) and ventral (d) views of NSM.PM 7387 from loc. PM 3002, ×1.2.

Plate 3

Fig. 1. Lateral (a) and frontal (b) views of NSM.PM 9248 from loc. PM 3F30, ×1.2.
Fig. 2. Lateral view of NSM.PM 7302 from loc. PM 3F26, ×1.2.
Fig. 3. Lateral view of NSM.PM 7053 from loc. F1, ×1.2.
Fig. 4. Lateral (a) and ventral (b) views of NSM.PM 7304 from loc. PM 3F26, ×1.2.
Fig. 5. Ventral (a) and lateral (b) views of NSM.PM 7335 from loc. PM 3F29, ×1.2.
Fig. 6. Lateral (a) and ventral (b) views of NSM.PM 7344 from loc. PM 3F24, ×1.2.
Fig. 7. Lateral (a, c) and ventral (b) views of NSM.PM 7336 from loc. PM 3F29, ×1.2.

Plate 4

Fig. 1. Lateral (a, c), frontal (b) and ventral (d) views of NSM.PM 7000 from loc. PM 3F16, ×0.9.
Fig. 2. Lateral (a, c), and ventral (b) views of NSM.PM 7047 from loc. PM 3F16, ×0.9.
Fig. 3. Lateral (a, c), and ventral (b) views of NSM.PM 7051 from loc. PM 3F17, ×0.9.

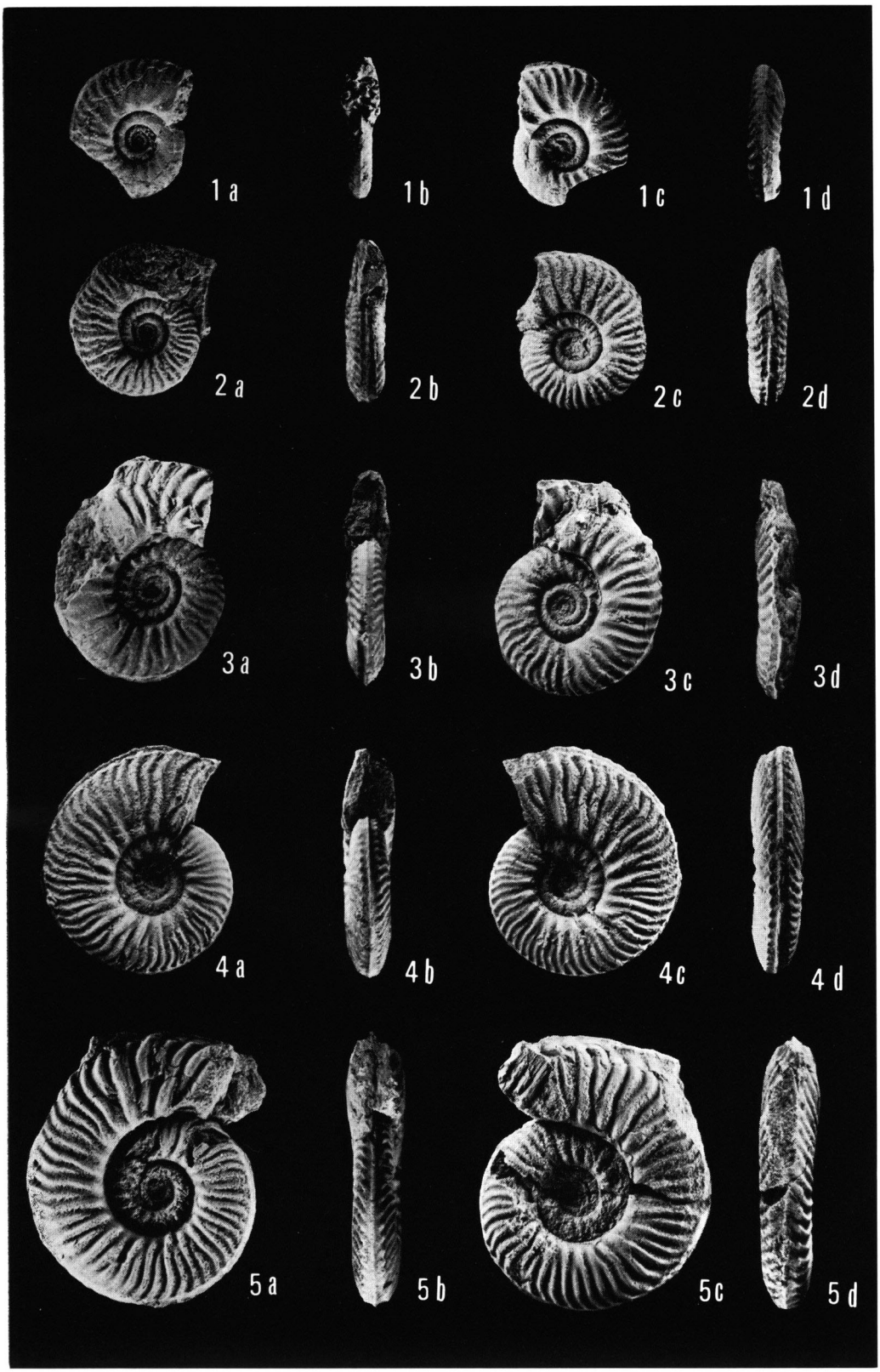
1a
1b
1c
1d
2a
2b
2c
2d
3a
3b
3c
3d
4a
4b
4c
4d
5a
5b
5c
5d

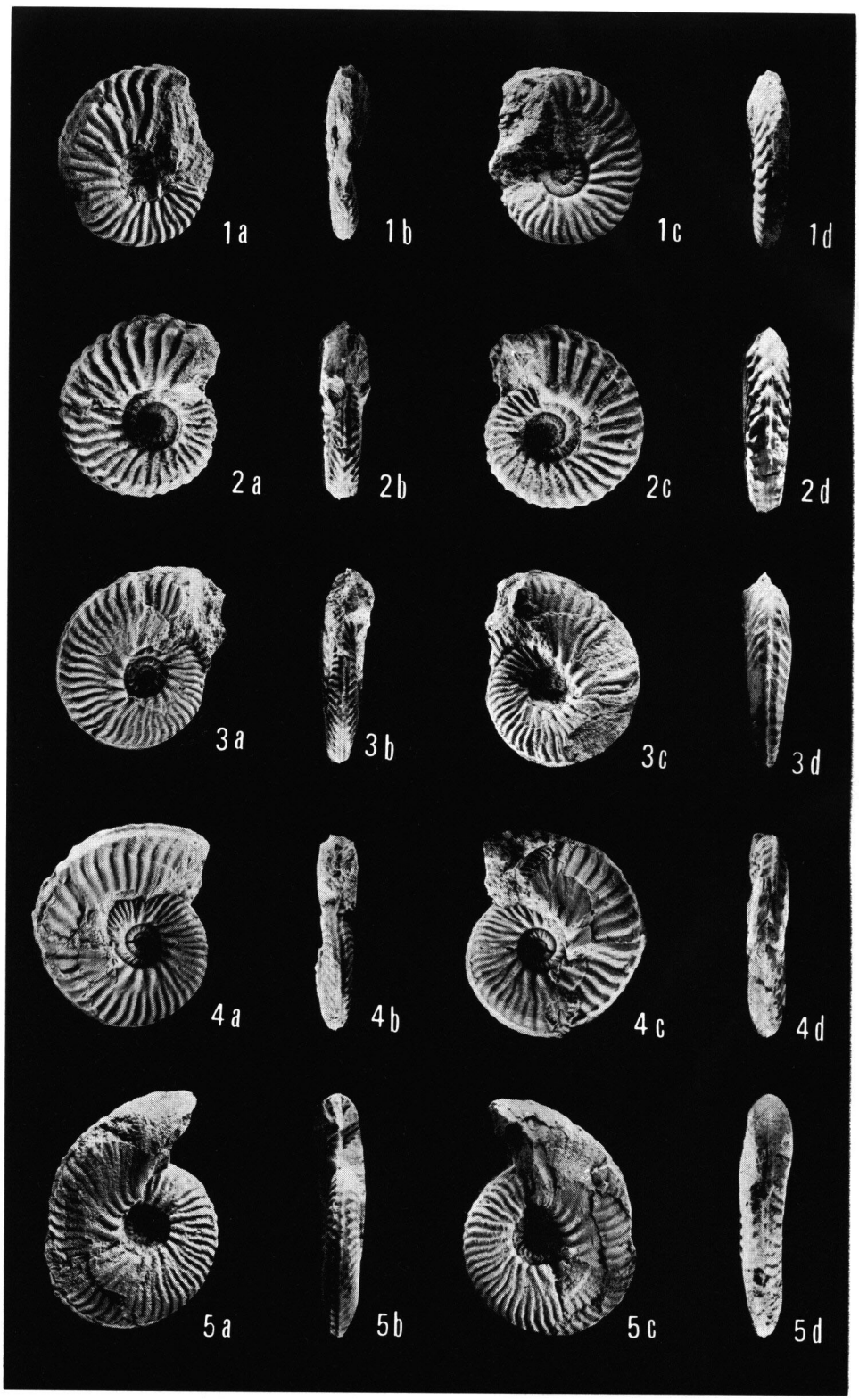
1a
1b
1c
1d
2a
2b
2c
2d
3a
3b
3c
3d
4a
4b
4c
4d
5a
5b
5c
5d

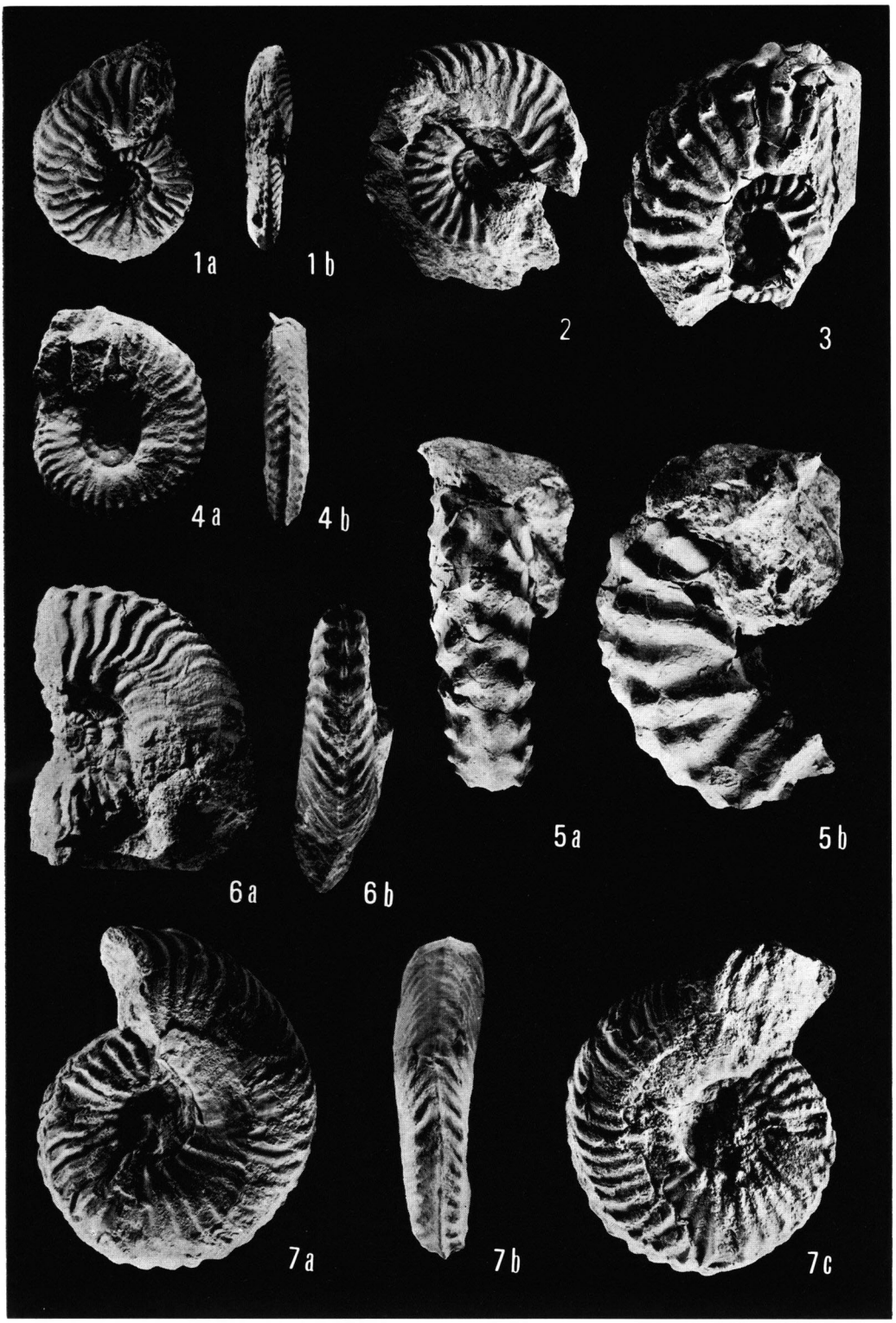
1a
1b
2
3
4a
4b
5a
5b
6a
6b
7a
7b
7c

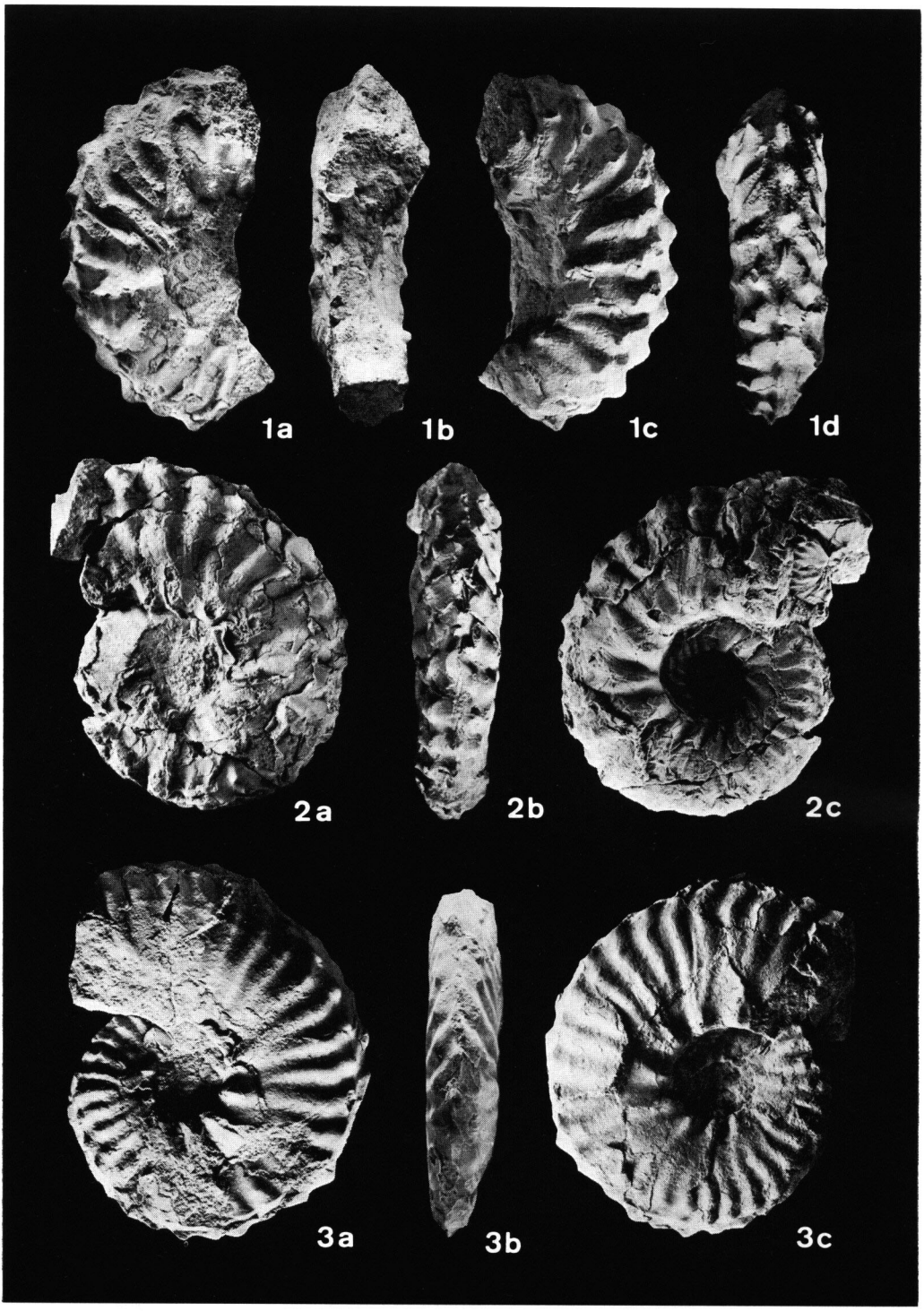
1a
1b
1c
1d
2a
2b
2c
3a
3b
3c